People's Democratic Republic of Algeria
Ministry of Higher Education and Scientific Research

University M'Hamed BOUGARA – Boumerdes

Institute of Electrical and Electronic Engineering
Department of Power and Control

Final Year Project Report Presented in Partial Fulfilment of the Requirements for the Degree of

MASTER

In **Power Engineering**

Option: **Power Engineering**

Title:

Solar Water Pumping

Presented by:

- **AGAB Djamel**
- **HATTOUM Abdelhak**

Supervisor:

Dr .METIDJI Brahim

Co-Supervisor:

Dr .MEDJOUDJ Rafik

Registration Number:……/2018

Dedication

I dedicate this modest work to our dear parents, our brothers and to all our family and friends

All our Teachers from primary school to our last year of university.

Djamel , Abdelhak

,

Acknowledgements

In the name of Allah the Most Beneficent and the Most Merciful, we thank Allah for all His blessing and strength that He gives us in completing this modest project

Secondly , We would like to thank our project supervisors, ***Dr. B.Metidji*** and **Dr. R. Medjoudj** *for all helps, assistance, and valuable feedback in the realization of this senior design project.*

A final thank you goes to our families and friends for their presence, support, and help.

Abstract

In this work, three-phase double stage water-pumping photovoltaic system using current control inverter is simulated using Matlab/Simulink. To deal with varying irradiance conditions, the Perturb and Observe (P&O) MPPT has been used. The main part of the project that is the control of AC motor using hysteresis field oriented control method has been implemented.

The proposed system consists of two-level inverter, the converter used is a Voltage Source Inverter (VSI) which is controlled using synchronous d-q reference frame to inject a controlled current into the AC induction motor .

Table of contents

Chapter Two: Modeling of Two-Level Inverter

Chapter Three: Three Phase Induction Motor

Chapter Four: Simulation and Results

Chapter five: Implementation

List of Figures

Chapter one: Modeling of PV Generator

Chapter Two: Modeling of Two Level Inverter

Chapter Three : Three Phase Induction Motor

Chapter Four: Simulation and Results

Chapter Five: Implementation

List of Tables

LIST OF ABBREVIATION

PV : Photo voltaic

DC : Direct Current

AC : Alternative Current

MPPT : Maximum Power Point Tracking

P&O : Perturb and Observe

VSI : Voltage Source Inverter

CSI : Current Source Inverter

PWM : Pulse Width Modulation

IM : Induction Motor

DE : Drive End

NDE : Non-Drive End

EMF : Electro-Magnetic Force

MMF : Magneto Motive Force

FOC : Field Oriented Control

PI : Proportional Integrator

GPIO: General Purpose Input Output

ADC: Analog to Digital Converter

General Introduction

The energy demand increases with the same rate as the population increase as well as the technology development. Besides exhausting of fossil fuels and negative effects of nuclear fuels, tendency of generation energy nearby location, where it is consumed, to decrease the transmission losses and improve the energy reliability has increased interest on renewable energy sources(RESs) [1].

Solar energy is one of the most important renewable energy with its superior advantages such as being inexhaustible energy source, accessible nearly all around the world, pollution free operation and little maintenance requirement. Solar energy is converted to DC electrical energy via photovoltaic (PV) modules. Since most of the loads are AC, an inverter is required. This PV system can operate either in standalone mode or grid interactive mode. The stand-alone PV system is economically superior in which other energy sources are impossible or difficult to use. In water pumping operation mode battery groups are not necessary, therefore the cost and size of the system are reduced [2 - 3].

Water-pumping PV systems seem to be an efficient solution to the environmental problems with their decreasing costs. However energy conversion efficiency of the PV systems is still low and this subject attracts many researchers interesting. In addition, it is important to operate PV energy conversion systems near the maximum power point to increase the output efficiency of PV arrays. Thus, power electronics inverters are required for maximum power point tracking (MPPT) algorithm, which provides maximum PV power. They are also needed for transferring the PV power to the ac loads. For this reason, in this work a three-phase double stages water pump interactive inverter with maximum power point tracking capability is simulated and part of the system is implemented. The details description of this project is compiled:

Chapter 1: A general introduction of PV systems is presented and mathematical model of PV cell is investigated.

Chapter 2: Describes the two-level three phase inverters with SVM control.

Chapter 3: presents induction motor with field oriented control using and describes the different types of water pumps .

Chapter 4: Simulates our system using Matlab/Simulink.

Chapter 5: Implementation of the main part of the implementation

Finally, the report terminates with a general conclusion.

Chapter One

Modeling of PV Generator

1.1 Introduction

Photovoltaic energy offer consumers the ability to generate electricity in a clean, quiet and reliable way. Photovoltaic systems are comprised of photovoltaic cells. The word photovoltaic comes from "**photo**," meaning light, and "**voltaic**," which refers to producing electricity. Therefore, the photovoltaic process is "producing electricity directly from sunlight." Photovoltaic are often referred to as PV.

Modeling this device necessarily requires taking data (irradiance and temperature) as input variables. The output can be current, voltage, power or other. However, plotting the I (V) or P (V) characteristics needs these three variables. Any change in the entries immediately implies changes in outputs. That is why, it is important to use an accurate model for the PV module.

This chapter will be devoted to modeling and studying the operation of PV cells and modules. As a first step, a PV model will be implemented using MATLAB/Simulink.

Finally, the effect of temperature and irradiance on the module performances will be visualized.

1.2 Types of PV systems

Solar PV system has been implemented for the daily usage which consists of different types of consumers. Practically there are two types of solar PV system; which are stand alone system and grid connected system. The consumer can choose the type of system based on their need and availability, and we can see in the following diagram the classification of Photovoltaic System types: [4]

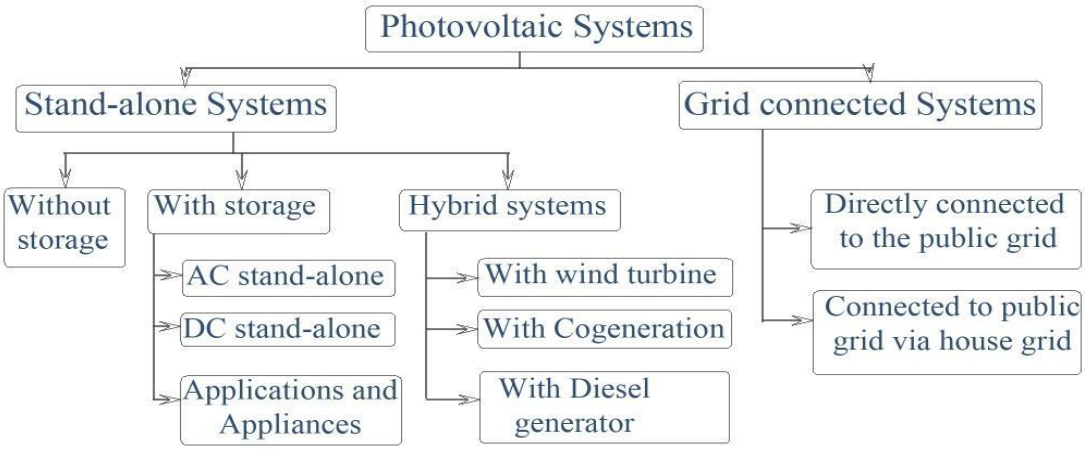

Figure 1.1: Classification of Photovoltaic System

1.2.1 Stand Alone PV Systems

Stand-alone PV systems are designed to operate independent of the electric utility grid, and are generally designed and sized to supply certain DC and/or AC electrical loads. [4]

1.2.1.1 Direct-Coupled PV System

The simplest type of stand-alone PV system is a direct-coupled system, where the DC output of a PV module is directly connected to a DC load .

In direct-coupled systems, the load only operates during sunlight hours. The common applications for this system are such as ventilation fans, water pumps and small circulation pumps for solar thermal water heating systems.

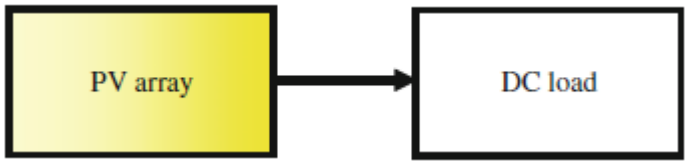

Figure 1.2: Direct-Coupled PV System**.** [4]

1.2.1.2 Stand-Alone PV System with Battery Storage Powering DC and AC Loads

In standalone PV applications, electrical power is required from the system during night or hours of darkness. Thus the storage must be added to the system. Generally, batteries are used for energy storage. Several types of batteries can be used such as lead-acid, nickel–cadmium, lithium zinc bromide, zinc chloride and vanadium batteries.

The inverter uses an internal frequency generator to obtain the correct output frequency.

A charge controller must keep the battery at the highest possible state while protecting it from overloaded by the photovoltaic generator and from over-discharge by loads. There are several types of charge controller

• **Shunt controller:** the function is to regulate the charging of battery. This controller is basically connected in parallel with array and battery.

• **Series controller:** this controller is commonly used in small PV system and connected in series between PV array and battery.

• **Tracking controller:** This controller tracks the maximum power point of PV array .

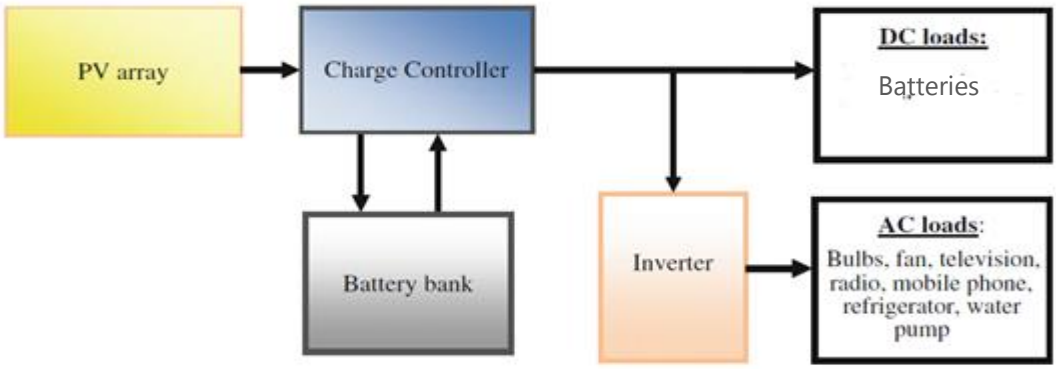

Figure 1.3: Stand-alone PV system with battery storage powering DC and AC loads [4]

1.2.1.3 Advantages of Stand-Alone PV System

The most important advantages of PV system are :

- The reliable supply of the load with electricity during operating time, a long lifetime,
- Expenses for maintenance must be low.

1.2.2 Grid-Connected PV Systems

Utility-interactive PV power systems mounted on residential and commercial buildings are likely to become important source of electric generation. Grid connected PV systems offer the opportunity to generate significant quantities of high-grade energy near the consumption point, avoiding transmission and distribution losses. These systems operate in parallel with existing electricity grids, allowing exchange of electricity to and from the grid. Grid-connected PV system can be subdivided into two systems: [4]

- Decentralized grid-connected PV systems
- Central grid-connected PV systems.

1.2.2.1 Decentralized Grid-Connected PV Systems

In these systems, energy storage is not necessary because solar radiation provides power in the houses and if there is surplus energy it can be injected into the grid. In this case, the inverter must integrate harmoniously with the energy (voltage and frequency) provided by the grid. During night or at instants when the PV power is inadequate, the grid can be used as a storage system and will feed the houses.

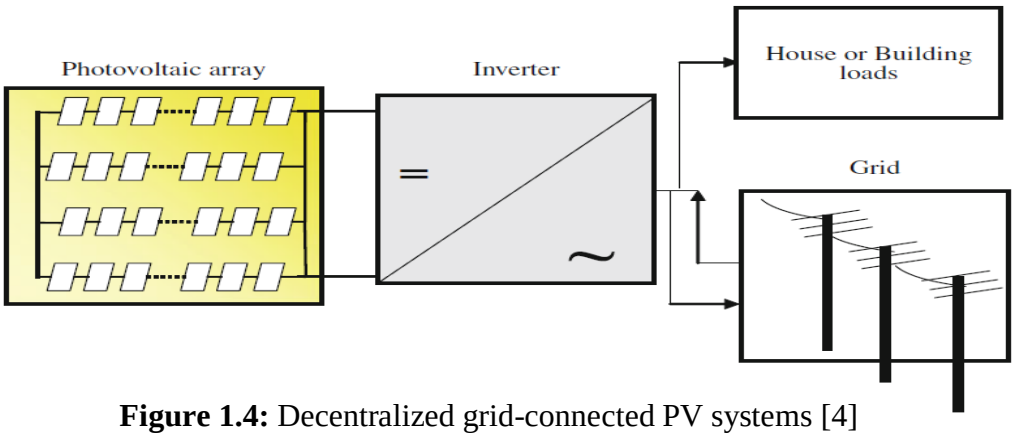

Figure 1.4: Decentralized grid-connected PV systems [4]

1.2.2.2 Central Grid-Connected PV Systems

It is a central photovoltaic power station and it is installed to systems up to the MW range. With this system, we can obtain medium or high voltage grid.

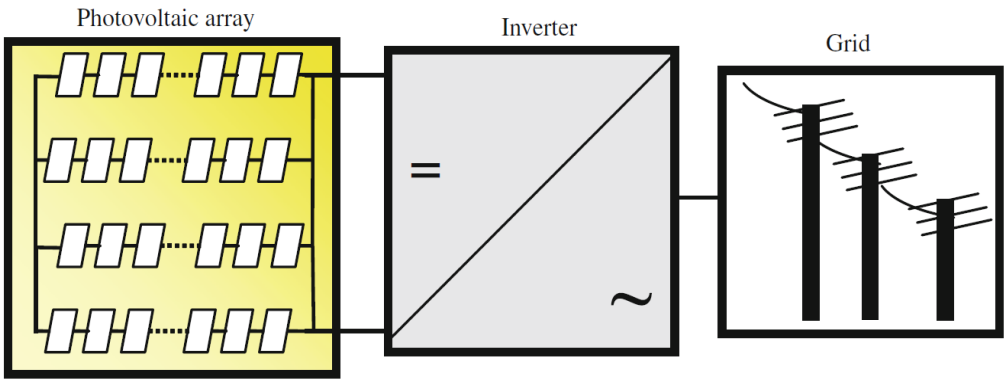

Figure 1.5: Central grid-connected PV systems [4]

1.2.3 Hybrid-Connected Systems

In the hybrid-connected system, more than one type of electricity generator is employed. The second type of electricity generator can be renewable, such as a wind turbine or conventional, such as a diesel engine generator. The diesel engine generator can also be a renewable source of electricity when the diesel engine is fed with biofuels. In this system both DC and AC loads can be satisfied simultaneously.

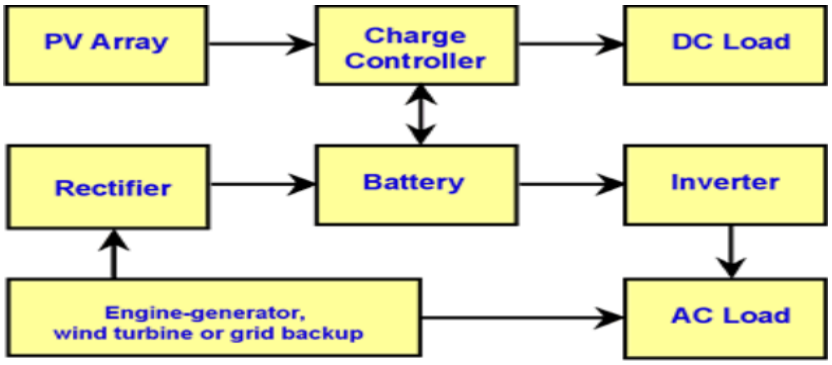

Figure 1.6: Hybrid-Connected Systems

1.3 The Photovoltaic system

PV systems are designed around the PV cell. Since a typical PV cell produces less than 5 W, cells must be connected in series-parallel configurations to produce enough power for high-power applications.

1.3.1 The PV cell

PV cells are made of semiconductor materials, such as silicon. For solar cells, a thin semiconductor wafer is specially treated to form an electric field. When light energy strikes the solar cell, electrons are knocked loose from the atoms in the semiconductor material. If electrical conductors are attached to the positive and negative sides, forming an electrical circuit, the electrons can be captured in the form of an electric current - that is, electricity. This electricity can then be used to power a load.

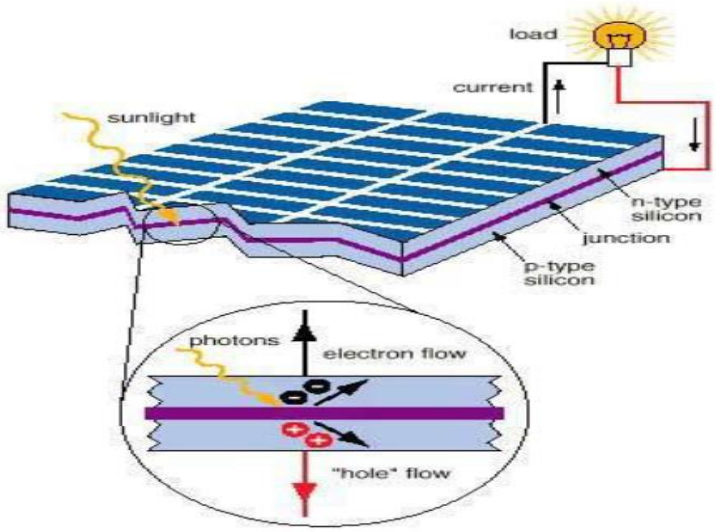

Figure 1.7: Basic Structure of PV Cell

1.3.1.1 Operation principle

When the photon of the solar radiation with an energy level above the material band gap strikes the solar cell, it creates an electron-hole pair, these pairs is generated at both sides of the p-n junction. The minority carriers (electrons in the p-side and holes in the n-side) are defused to the junction and swept away in the opposite direction (electrons to the n-side and holes to p-side) by the electric field, generating a current in the cell, this may be further illustrated by the **figure 1.7.**

Metallic contacts are added at both sides to collect the electrons and holes and the current can flow. But in the case of the n-type layer which faces the sun light the contacts are made as strips to allow the solar light to pass and they are called fingers.

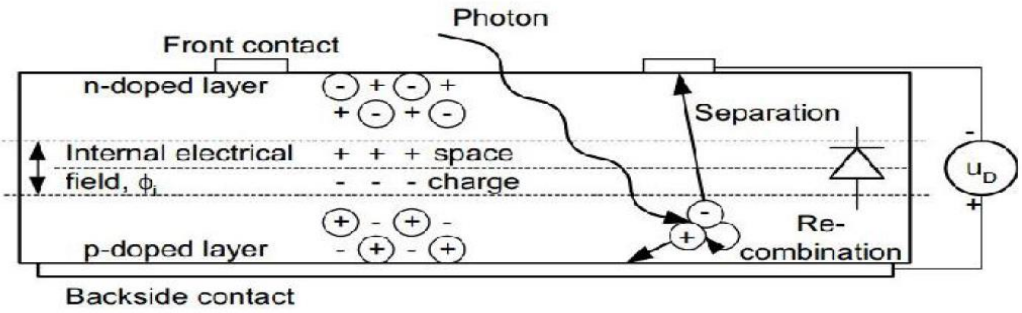

Figure 1.8: Operation principle of PV Cell

1.3.2 The PV MODULE

Due to the low voltage generated in a PV cell (around 0.5V), several PV cells are connected in series (for high voltage) and in parallel (for high current) to form a PV module for desired output. Separate diodes may be needed to avoid reverse currents, in case of partial or total shading, and at night. The p-n junctions of silicon cells may have adequate reverse current characteristics and these are not necessary. Reverse currents waste power and can also lead to overheating of shaded cells. Solar cells become less efficient at higher temperatures and installers try to provide good ventilation behind solar panels.

1.3.3 The PV ARRAY

The power that one module can produce is not sufficient to meet the requirements of home or business. Most PV arrays use an inverter to convert the DC power into alternating current that can power the motors, loads, lights etc. The modules in a PV

array are usually first connected in series to obtain the desired voltages; the individual modules are then connected in parallel to allow the system to produce more current.

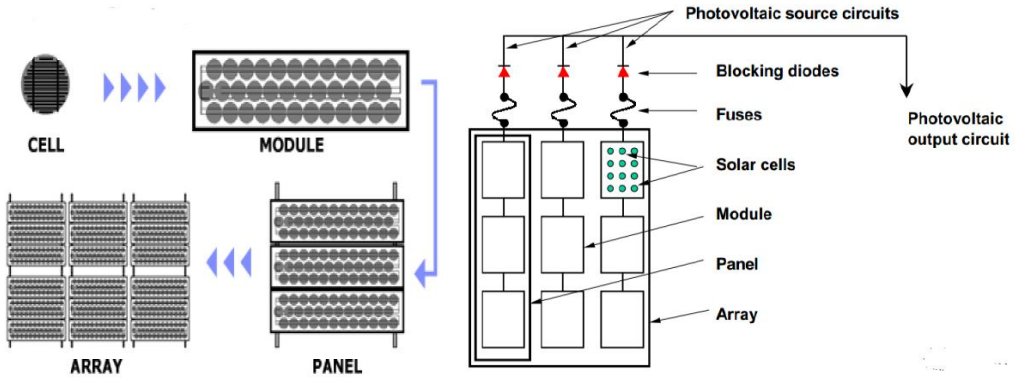

Figure 1.9: The whole PV system

1.4 Modeling of PV cell

As the solar cell shows a nonlinear (I-V) characteristic curve, many models for the equivalent circuit were suggested in the aim of explaining this nonlinear behavior (Single-diode model, Double-diode model and the simplified model).

The single-diode model with its two versions (depending of the shunt resistance, if it's taken in consideration or not) as shown in the two below figures, is the most used model in PV cell simulation as they offer a good compromise between complexity and the quality of the gotten results compared to the real ones. [5][6]

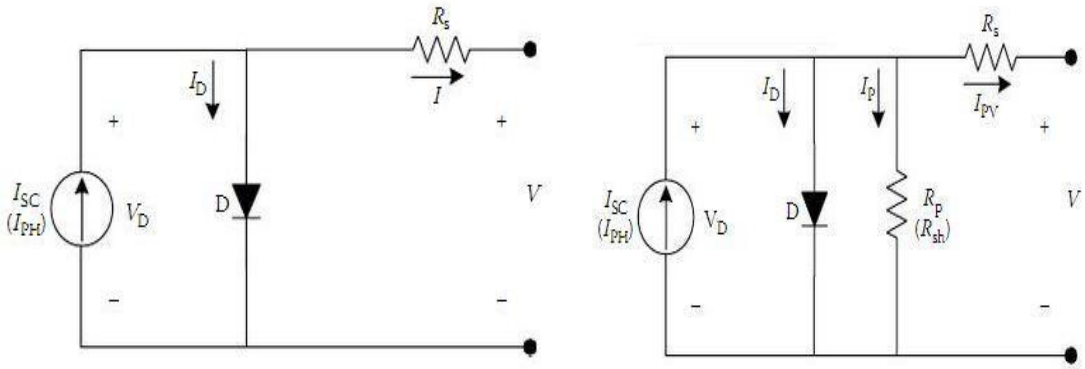

(a) **(b)**

Figure 1.10: (a) -Single diode with ***Rs***. **(b)** Single diode with ***Rs*** and ***Rsh***

The cell output current can be obtained simply by applying Kirchhoff's law to the circuit in the figure 1.9(b) as follows:

$$I_{PV} = I_{ph} - I_D - I_{sh} \quad (1.1)$$

Then the I-V characteristics of the PV cell are described by:

$$I_{ph} = \frac{G}{Gref} I_{sc,ref} + KI\,(T_c - T_{c,ref})) \quad (1.2)$$

$$I_D = I_0\left[\left(e^{\frac{q(V+Rs\,X\,I)}{AKTc}}\right) - 1\right] \quad (1.3)$$

$$I_0 = I_{0,ref}\left(\frac{Tc}{Tc,ref}\right)^3 e^{\left(\left(\frac{q.Eg}{A.K}\right)\left(\frac{1}{Tc,ref} - \frac{1}{Tc}\right)\right)} \quad (1.4)$$

$$I_{0,ref} = \frac{I_{sc,ref}}{e^{\left(\frac{Voc,ref}{A.K.Tc}\right)} - 1} \quad (1.5)$$

$$I_{sh} = \frac{V - Rs\,X\,I}{R_{sh}} \quad (1.6)$$

Then, the equation **(1.1)** can written in more details after substituting **(1.2)**, **(1.3)** and **(1.6):**

$$I_{PV} = \frac{G}{Gref} I_{sc,ref} + K_I\,(T_c - T_{c,ref})) - I0\left[\left(e^{\frac{q(V+Rs\,X\,I)}{AKTc}}\right) - 1\right] - \frac{V - Rs\,X\,I}{Rsh} \quad (1.7)$$

Where:

I_{ph} : The light or the photo current.

I_D: The diode current.

I_{sh}: The current in parallel resistor.

K: Boltzmann's constant = 1.38×10^{-23} J/◦K

q: The charge of an electron = 1.6×10^{-19} C.

A: The diode ideality factor.

E_g: The band gab energy for the semiconductor.

T_c: Cell operation temperature.

$T_{c,f}$: Cell temperature at STC.

G: The intensity of solar irradiance, W/m^2.

I_{ph}, : The reference short circuit current.

I0 : The reverse saturation or leakage current of the diode.

$I_{0,ref}$: The reference reverse saturation current.

K_I : The temperature coefficient of short-circuit current (A/°K).

1.5 Effect of temperature and irradiance on PV module

Photovoltaic performance is affected by external factors which include temperatureand irradiation. These two parameters are dependent on the geographical area of installation and the different year's seasons.

1.5.1 Effect of temperature

Like all other semiconductor devices, solar cells are sensitive to temperature, which directly affects the amount of power produced by the solar module. The most affected parameter by a variation in temperature is the open-circuit voltage, and an increase in temperature will decrease the voltage. The impact of the temperature on the PV module is shown in **figure 1.10**.

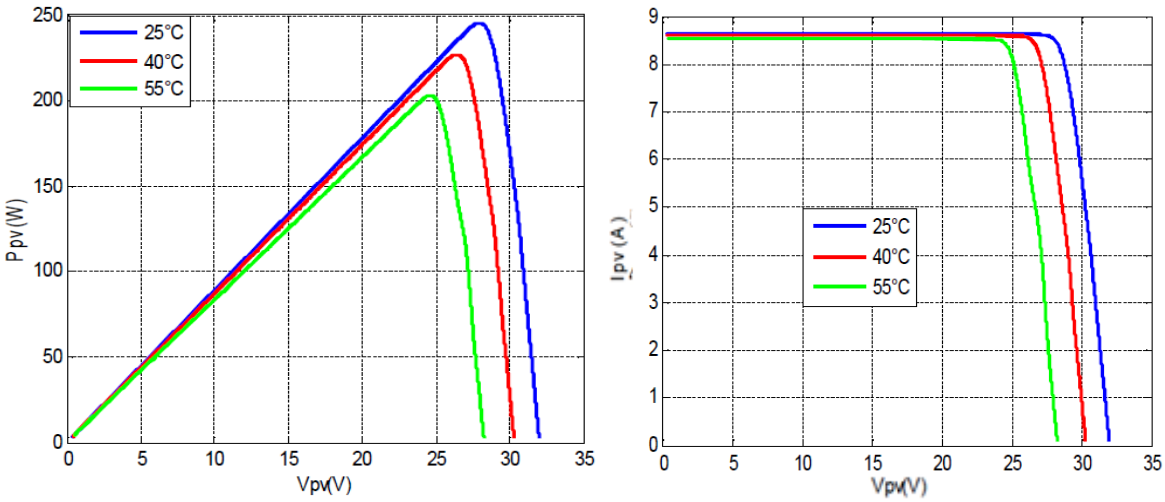

Figure 1.11: Effect of temperature variation on the I-V and P-V characteristics.

1.5.2 Effect of irradiance

The irradiance affects the short circuit current (Isc) which is proportional to it. The power produced by the PV cell is the product of voltage and current P=I.V. Because of this relationship, the net effect of an increase in irradiance is an increase in power

production. Hence, solar cells work best with higher levels of irradiance. The impact of the irradiance on the PV module is shown in **figure 1.11**.

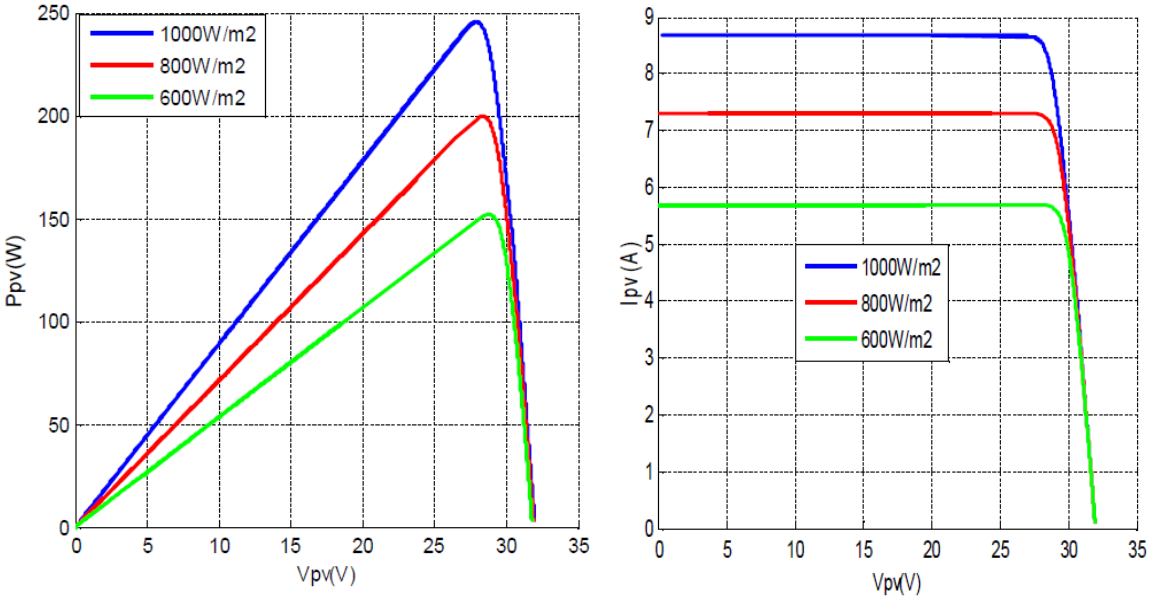

Figure 1.12: Effect of irradiance variation on the I-V and P-V characteristics.

1.6 Maximum Power Point Tracking algorithms

As we know MPPT algorithms are necessary in PV applications because the MPP of solar panel varies with irradiance and temperature. So the use of MPPT algorithm is required in order to obtain maximum power from the solar array.

Over the last decades many techniques to find the MPP have been developed and published, such as Perturb and Observe, Incremental conductance... These techniques differ in many aspects such as the complexity, cost, and convergence speed

In this part, we will present the Perturbe and Observe.

1.6.1 Perturb and observe (P&O):

The P&O technique involves a perturbation in the duty cycle of the power converter (DC/DC converter), the sign of the last perturbation and the sign of the last increment in the power decide what the next perturbation should be. Such that if there is an increment in the power, the perturbation should be kept in the same direction and if the power decreases, then the next perturbation should be in the opposite direction.

Based on these facts, the algorithm is simulated using Matlab/Simulink, a scheme of the algorithm is shown in the **figure1.13**

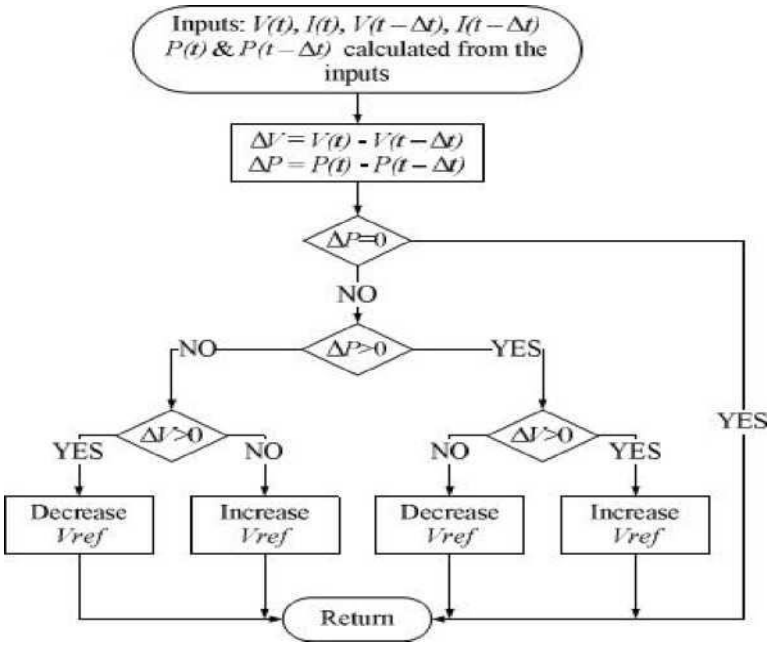

Figure 1.13: Flowchart of the P&O algorithm.

1.7 Conclusion

This chapter was dealt with PV generators, which can be found in different types of systems: stand-alone, grid-connected or hybrid. The heart of these systems is the PV cell and module. The model of the PV cell and module has been presented, and the effect of climate condition on the main parameters, voltage, current and power has been analyzed.

Then the Perturb and Observe MPPT method was presented and analyzed.

Chapter Two

Modeling of Two-Level Inverter

2.1 Introduction

A power electronics device which converts DC power to AC power at required magnitude (V), frequency (Hz) is known as an inverter. There are two common types of inverters, voltage source inverters (VSI) when the inverter has a DC source with small or negligible impedance and current source inverters (CSI) when the input DC source has a high impedance.

Three major classes of regulators have been developed over last few decades: hysteresis regulators, linear PI regulators and predictive dead-beat regulators. [7]

Among the various PWM technique, the hysteresis band current control is used very often because of its simplicity of implementation. Also, besides fast response current loop, the method does not need any knowledge of load parameters.

In this chapter a two-level inverter is firstly discussed. Secondly, based on the topological structure of two-level inverter, and the method of hysteresis current control is proposed .At last, the proposed control method is programmed with Matlab/Simulink.

2.2 Two-level inverter

A three phase inverters are used to provide industrial applications by adjustable frequency power. A six steps bridge is used for three phase inverter by using six switches, two switches for each phase.

2.2.1 Structure of Two-level inverter

The diagram of a three-phase two-level voltage source inverter is shown in **Figure 2.1**.

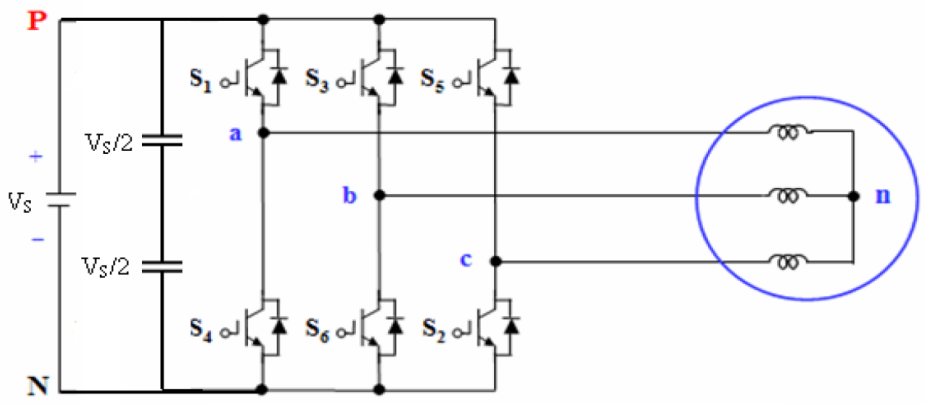

Figure 2.1 : Three phase inverter [8]

The operating status of the switches in the two-level inverter in **Figure 2.1** can be represented by switching states. As indicated in **Table 2.1**, switching state '1' denotes that the upper switch in an inverter leg is ON and the inverter terminal voltage (Van, Vbn, Vcn) is positive , while '0' indicates that the inverter terminal voltage is zero due to the conduction of the lower switch. [9]

Table 2.1 : Switching states for a three-phase two-level inverter

	Leg a		Leg b		Leg c	
STATE	S1	S2	S3	S4	S5	S6
1	ON	OFF	ON	OFF	ON	OFF
0	OFF	ON	OFF	ON	OFF	ON

The inverter is composed of six switches, S1 to S6 where the output voltage for each leg, Van, Vbn, Vcn, depends only on Vs and the switch status.

Figure 2.2 shows a graphical view of the line-to-line voltage VAB

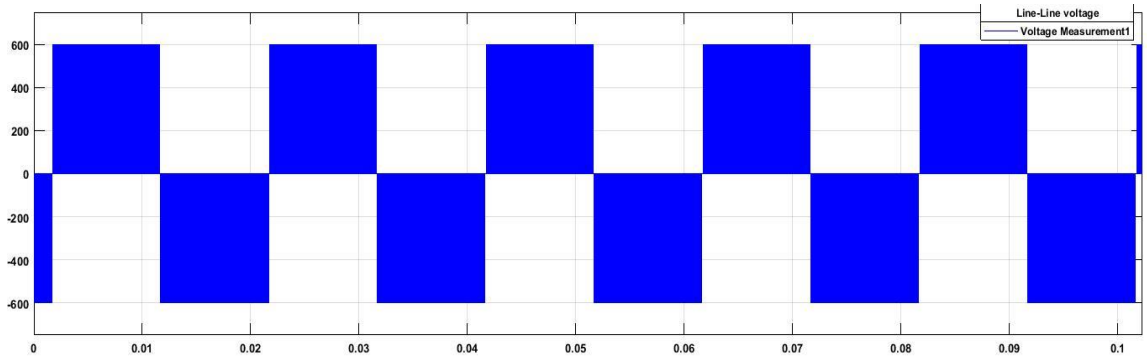

Figure 2.2: The output line to line voltage for three phase two level inverter, Vdc=600v

2.2.2 Open-Loop Modulation of Two-Level Inverters

The fundamental concept of PWM is to control the duty cycle of each switch (mark-space ratio or ON time) at a high switching frequency to generate a train of switched pulses that have the required low frequency fundamental component. [10]

The second objective of these strategies is to arrange the switching pulses in such a way as to minimize unwanted harmonic distortion, switching losses or to manage secondary performance criteria (e.g. common mode voltage). The most common modulation strategy

for a two-level voltage source inverter is naturally sampled sine-triangle pulse width modulation, shown in **Figure 2.3**.

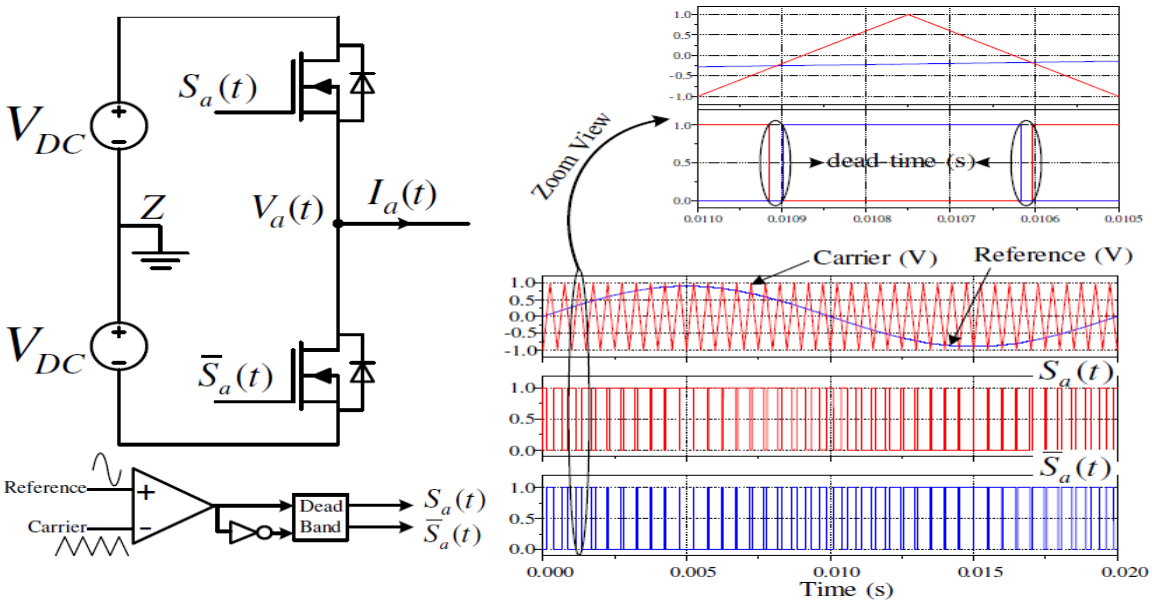

Figure 2.3: Open-loop modulation of two-level single phase leg voltage source inverter [10]

In this strategy, a low frequency sinusoidal reference signal (the modulation command) is compared against a high frequency triangular carrier. When the reference signal is greater than the carrier signal, the VSI phase leg upper switch turns ON, the lower switch is turned OFF, and the inverter phase leg output switches to the upper DC bus voltage. When the reference signal is smaller than the carrier signal, the VSI phase leg lower switch turns ON, the upper switch turns OFF, and the inverter phase leg output switches to the lower DC bus voltage.

For a voltage source inverter, the switches of each phase leg cannot be turned ON simultaneously, a short null period is introduced between the turn OFF and turn ON events of the phase leg switches. This short period (usually a few percent of the switching period) is called dead-time and is essential for any VSI modulation strategy. Once the modulation of a two-level half-bridge VSI is established, the concept can be easily extended to the full-bridge single-phase and three-phase VSIs. **Figure 2.4** shows open-loop naturally sampled sine-triangle PWM for a single-phase VSI and the switching arrangement to achieve a two-level output voltage. It has been shown that the optimum harmonic performance of a

single-phase H-bridge is achieved using a three-level double-edge asymmetrically sampled PWM. In this way, each phase leg uses a common triangle carrier where their sinusoidal reference commands are displaced by 180°. This ensures the cancellation of the main carrier harmonics. [10]

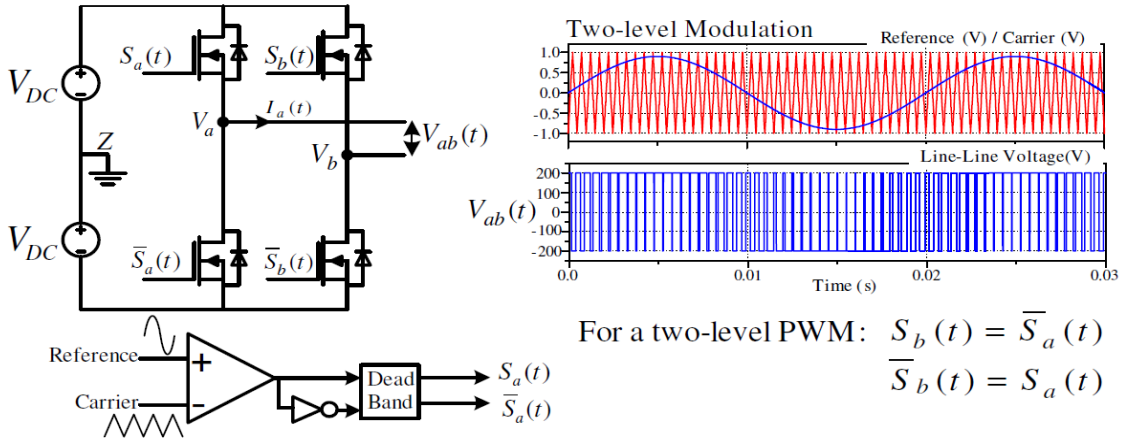

Figure 2.4: Open-loop modulation of full-bridge VSI using two-level sine-triangle PWM [10]

Figure 2.5 shows open-loop sine-triangle PWM of a two-level three-phase VSI with a separate modulation command (sinusoidal reference signal) per phase, to form a complete set of three-phase modulation commands that are now displaced by 120°. It also shows the switched phase *a* voltage and the three-level switched *ab* line to line voltage.

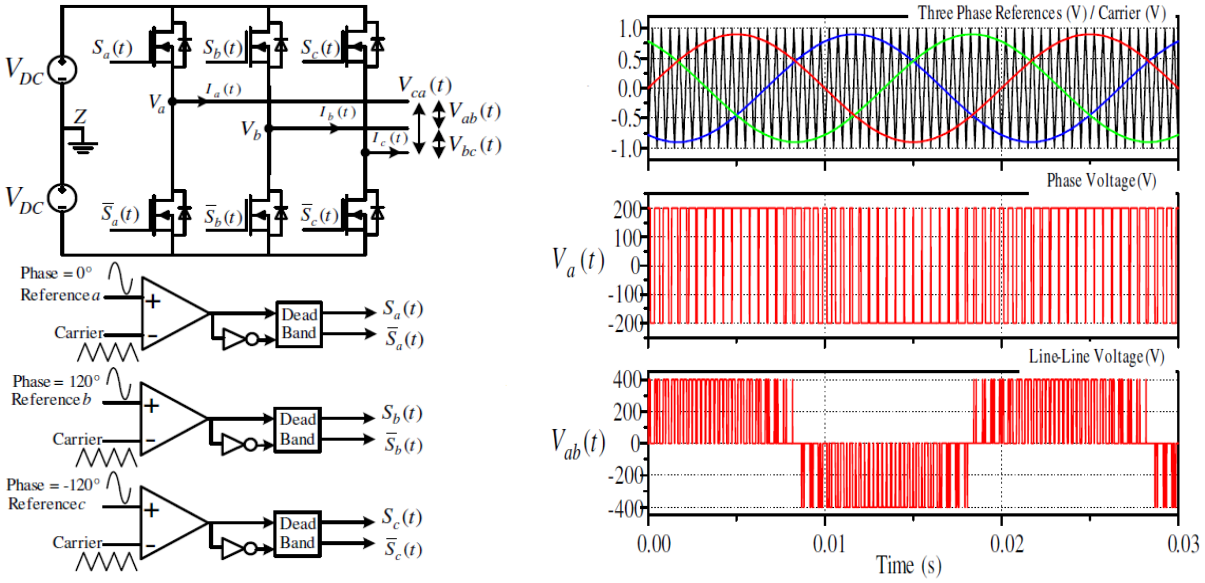

Figure 2.5: Open-loop modulation of two-level three-phase VSI using sine-triangle PWM [10]

2.3 Hysteresis Current Control Method

2.3.1 Principle of operation

Hysteresis current method limits the actual current between two boundaries equally displaced from the reference. It does not let the actual current to leave the band between the boundaries by turning the switches ON and OFF. The current error is obtained by subtracting the actual current from the reference current, shown by '' *ea* '' in **Figure 2.6**. Next, it is sent to the hysteresis block to become restricted between the mentioned boundaries, therefore the error can be controlled between desired values. Then, the output of the hysteresis block is applied for turning the switches ON and OFF.

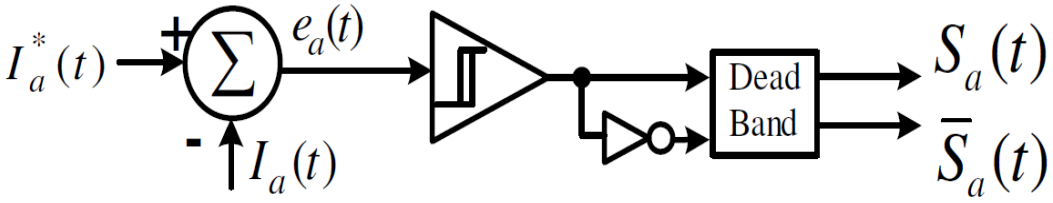

Figure 2.6: Basic topology of hysteresis band [10]

The reference current **Ia∗** is compared with the actual current in the hysteresis band. Basically the main principle of operation is as follows:

When the actual current increases and exceeds the prescribed hysteresis boundary, the upper switch would be turned OFF and the lower switch is turned ON. This means that the current is restricted by the upper boundary and it then starts to decay. When the actual current tends to decrease more than the lower boundary, the upper switch will be ON and the lower switch will be OFF to prevent this descent. Then the current starts to increase again. This process will be constantly repeated to keep the actual ripple in the desired range. This process is named the two-level hysteresis control, and is illustrated in **Figure 2.7:**

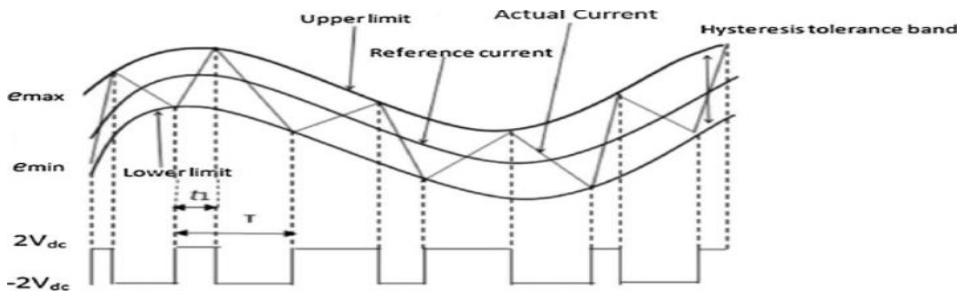

Figure 2.7: Two-level Hysteresis control

Hysteresis method is applied to three-phase in a similar way to the single phase system, but all phases should be under hysteresis control separately. The conditions for switching the devices are noted below:

$$\begin{cases} \text{Upper switch ON} \quad \text{or} \quad U=1 \quad \text{for} \quad (I^* - I) > HB \\ \text{Lower switch ON} \quad \text{or} \quad U=-1 \quad \text{for} \quad (I^* - I) < -HB \end{cases}$$

Where 'U' and 'HB' represent the output of the hysteresis block and the hysteresis bandwidth respectively.

2.3.2. Current controller

The current controller has direct influence on the drive performance and its design requires special considerations. The basic requirements for the current controllers are low harmonics to reduce losses, low torque pulsation, low noise in the motor and fast response in order to provide high dynamic performance. [10]

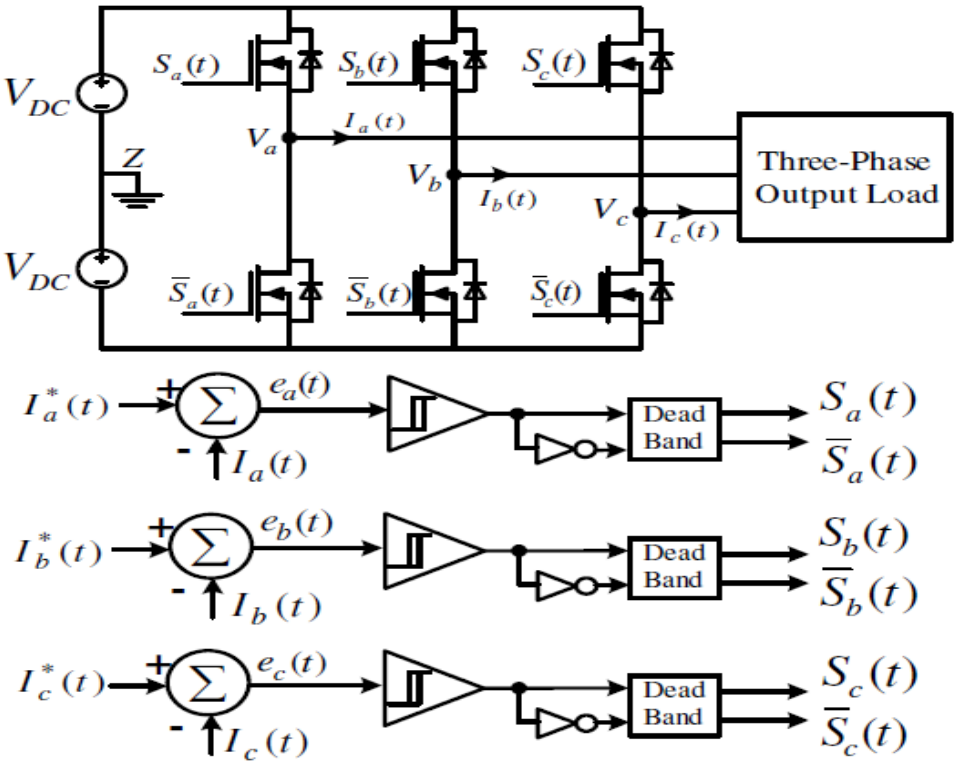

Figure 2.8: Hysteresis current controller. [10]

The logic operation of the voltage source inverter under current control is reported in **Table 2.2**. There are eight switch combinations for the six switches of the inverter. The voltage vectors corresponding to the active states are shown in **Figure 2.9**. The six commands V_1 to V_6 correspond to active voltage vectors, the remaining two V_0 and V_7 correspond to the zero voltage vectors.

In the hysteresis current controller of **Figure 2.8**, load currents I_a, I_b and I_c are respectively forced to follow reference currents I_{aref}, I_{bref} and I_{cref} within a hysteresis band by the switching action of the inverter.

The upper and lower bounds of the hysteresis band are set for the motor current, and the hysteresis controller logic control can be described according to the following rules.

Rule A:	**For**	$I_{aref} > 0$:	$\overline{Sa} = 0$,
	If	$I_a > I_{aref} + \Delta I$	***Then*** $Sa = 0$,
	Else if	$I_a < I_{aref} - \Delta I$	***Then*** $Sa = 1$,
	Else	no change.	
Rule B:	**For**	$I_{aref} < 0$:	$Sa = 0$,
	If	$I_a > I_{aref} + \Delta I$	***Then*** $\overline{Sa} = 1$,
	Else if	$I_a < I_{aref} - \Delta I$	***Then*** $\overline{Sa} = 0$,
	Else	no change.	

Table 2.2 : VSI conduction modes

State Order	Leg a		Leg b		Leg c		Operation Modes
	Sa	$\overline{Sa}$	Sb	$\overline{Sb}$	Sc	$\overline{Sc}$	
V_0	0	1	0	1	0	1	Freewheeling
V_1	1	0	0	1	0	1	Active
V_2	0	1	1	0	0	1	Active
V_3	1	0	1	0	0	1	Active
V_4	0	1	0	1	1	0	Active
V_5	1	0	0	1	1	0	Active
V_6	0	1	1	0	1	0	Active
V_7	1	0	1	0	1	0	Freewheeling

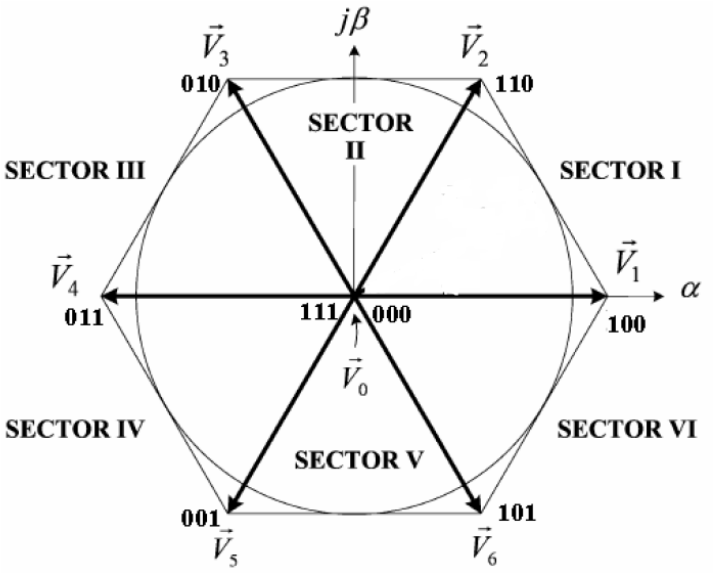

Figure 2.9: Switching states under current controller. [8]

2.4 Conclusion

This chapter provides a comprehensive analysis on the two-level inverter. A number of issues were investigated, including the inverter configuration, operating principle and Hysteresis Current Control technique and the performance of the three-phase two-level six switch inverter has been explained**.**

Chapter Three

Three Phase Induction Motor

3.1 Introduction

The induction motor is the most widely used AC machines in the industry worldwide because of its multiple well-known advantages: simple construction , good self-starting capability, robustness, low cost and effectiveness .

Its applications are various such as cooling fans, printing machines rolling mills and driving pumps .

Pumps are used to move or raise fluids. They are not only very useful, but are excellent examples of hydrostatics.

In this chapter, we present a review about the most relevant concepts of the induction motor, and we use the field oriented method to control the induction motor.

3.2 Three Phase Induction Motor

3.2.1 Structure of Induction Motor

The induction motor is a type of AC motor; it is called an induction motor because the working principles are based on electromagnetic induction .The structure of an IM is depicted in **Figure 3.1** [12]

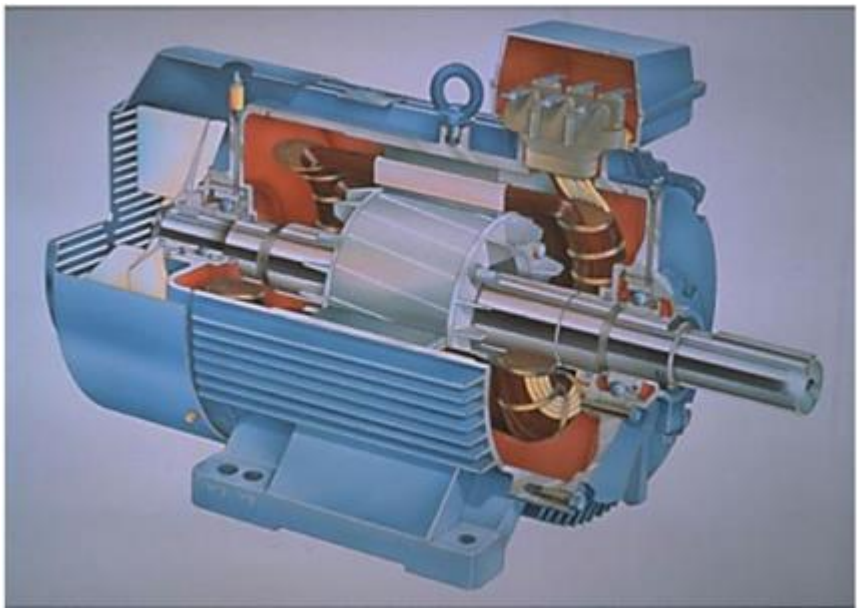

Figure 3.1: Cross section of the squirrel cage induction motor (copyright granted, ABB)

The AC induction motor comprises two electromagnetic parts:

- Stationary part called the stator,
- Rotating part called the rotor,

The stator and the rotor are each made up of an electric circuit, usually made of insulated copper or aluminum winding, to carry current, a magnetic circuit, usually made from laminated silicon steel, to carry magnetic flux

Stator :

The stator is the outer stationary part of the motor, which consists of:

- ✓ The outer cylindrical frame of the motor or yoke**,** which is made either of welded sheet steel, cast iron or cast aluminum alloy.
- ✓ The magnetic path**,** which comprises a set of slotted steel laminations called stator core pressed into the cylindrical space inside the outer frame. The magnetic path is laminated to reduce eddy currents, reducing losses and heating.
- ✓ A set of insulated electrical windings**,** which are placed inside the slots of the laminated stator. The cross-sectional area of these windings must be large enough for the power rating of the motor. For a 3-phase motor, 3 sets of windings are required, one for each 2 phase connected in either Star or Delta.

Details of construction of stator are shown in **Figure 3.2**.

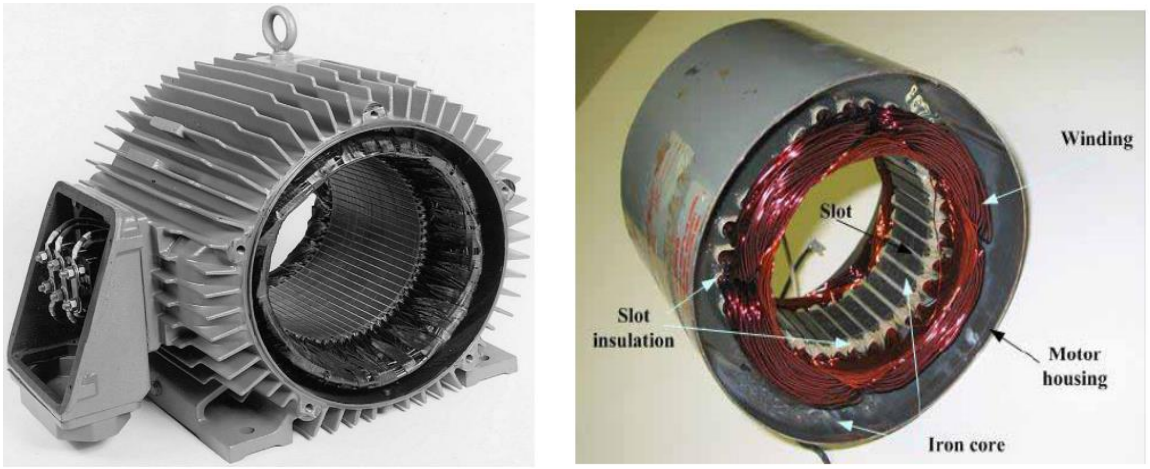

(a) **(b)**

Figure 3.2: (a) stator structure **(b)** Stator composition

Rotor

There are two different types of induction motor rotors which can be placed inside the stator. One is called a **cage rotor**, while the other is called a **wound rotor**.

Squirrel-Cage Rotor:

A cage induction motor rotor consists of a series of conducting bars laid into slots carved in the face of the rotor and shorted at either end by large shorting rings. This design is referred to as a cage rotor because the conductors, if examined by themselves, would look like one of the exercise wheels that squirrels or hamsters run all.

wound rotor:

A wound rotor has a complete set of three-phase windings that are similar to the windings on the stator. The three phases of the rotor windings are usually Y-connected, and the ends of the three rotor wires are tied to slip rings on the rotor's shaft. Wound-rotor induction motors are more expensive than cage induction motors, and they require much more maintenance because of the wear associated with their brushes and slip rings.

As a result, wound-rotor induction motors are rarely used.

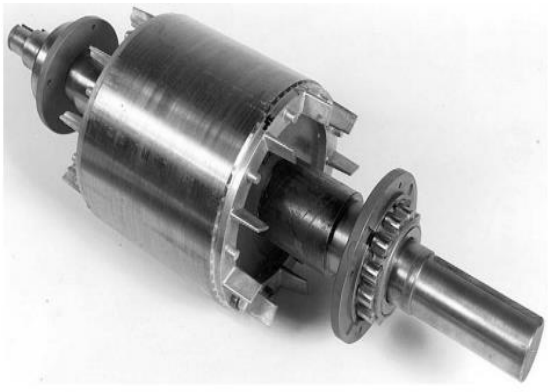

Figure 3.3: Squirrel-Cage Rotor

Figure 3.4: Wound Rotor

In addition to the rotor and stator , Induction motor is also composed of other parts as it is illustrated in **Figure 3.4** which are required in order to complete it . These parts are:

- **Two end-flanges** : to support the two bearings ,one at the drive-end (DE) and the other at the non drive-end (NDE)
- **Two bearings :** to support the rotating shaft ,at DE and NDE
- **Steel shaft** : for transmitting the torque to the load
- **Cooling fan:** located at the NDE to provide forced cooling for the stator and rotor
- **Terminal box** :on top or either side to receive the external electrical connections

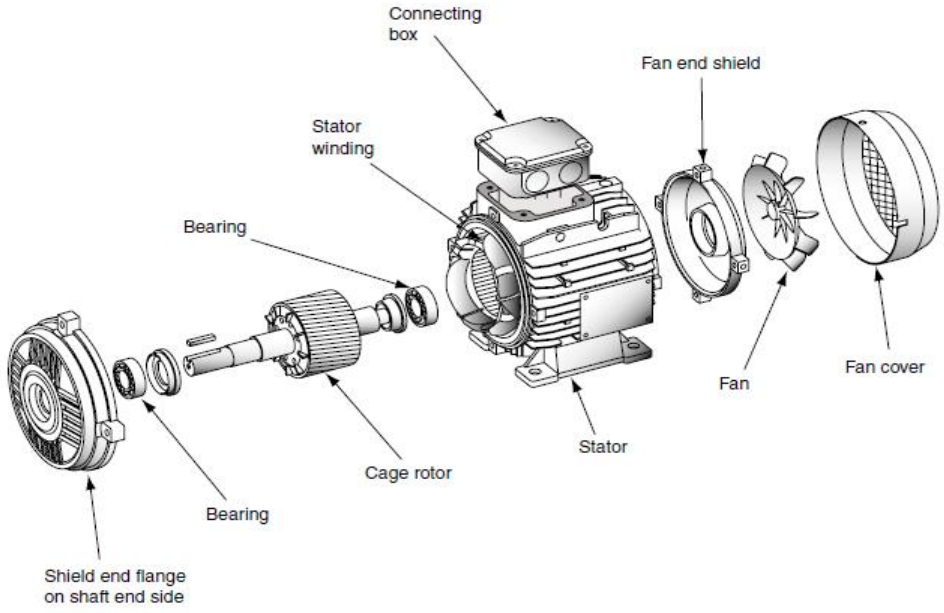

Figure 3.5: Assembly details of a typical AC induction motor

3.2.2 Principle of Operation:

Consider a portion of 3-phase induction motor as shown in **Figure. (3.1).** The operation of the motor can be explained as under:

- When 3-phase stator winding is energized from a 3-phase supply, a rotating magnetic field is set up which rotates round the stator at synchronous speed Ns(=120f/P).
- The rotating field passes through the air gap and cuts the rotor conductors, which as yet, are stationary. Due to the relative speed between the rotating flux and the stationary

rotor, e.m.f.s are induced in the rotor conductors. Since the rotor circuit is short-circuited, currents start flowing in the rotor conductors.

- The current-carrying rotor conductors are placed in the magnetic field produced by the stator. Consequently, mechanical force acts on the rotor conductors. The sum of the mechanical forces on all the rotor conductors produces a torque which tends to move the rotor in the same direction as the rotating field.
  - The fact that rotor is urged to follow the stator field (i.e., rotor moves in the direction of stator field) can be explained by Lenz's law. According to this law, the direction of rotor currents will be such that they tend to oppose the cause producing them. Now, the cause producing the rotor currents is the relative speed between the rotating field and the stationary rotor conductors. Hence to reduce this relative speed, the rotor starts running in the same direction as that of stator field and tries to catch it.
  -

3.3 Mathematical model of Induction Motor

To derive the mathematical model of induction motor the general electrical scheme of induction motor is very drawn. **Figure 3.6** illustrates the drawn electric scheme of an induction motor.

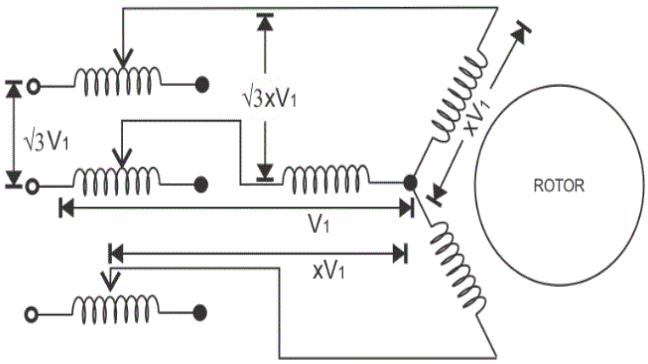

Figure 3.6: Electric scheme of an induction motor

In order to derive the mathematical equation of a three-phase induction motor, the following assumptions are made:

- The three-phase motor is symmetrical.
- Only the fundamental harmonic is considered, while the higher harmonics of the spatial field distribution and of the magneto-motive force (MMF) in the air gap are disregarded.
- The spatially distributed stator and rotor windings are replaced by a specially formed, so called concentrated coil.
- The effects of anisotropy, magnetic saturation, iron losses, and eddy currents are neglected.
- The coil resistances and reactance are taken to be constant
- In many cases, especially when considering steady state, the current and voltages are taken to be sinusoidal.

Taking into consideration the earlier-stated assumptions, the following equations of the instantaneous stator phase voltage values can be written as follows:

$$V_a = R_s i_a + \frac{d}{dt}\psi_a \quad (3.1)$$

$$V_b = R_s i_b + \frac{d}{dt}\psi_b \quad (3.2)$$

$$V_c = R_s i_c + \frac{d}{dt}\psi_c \quad (3.3)$$

Assuming that we have a three-phase balanced system meaning:

$$V_{a0} + V_{b0} + V_{c0} = 0 \quad (3.4)$$

3.3.1 D-Q model equations :

After applying the a-b-c / d-q transformation the motor mathematical model becomes as follow:

The stator voltage differential equations

$$V_{sd} = R_s i_{sd} + \frac{d}{dt}\psi_{sd} - w\psi_{sq} \quad (3.5)$$

$$V_{sq} = R_s i_{sq} + \frac{d}{dt}\psi_{sq} - w\psi_{sd} \quad (3.6)$$

The rotor voltage differential equations

$$V_{rd} = 0 = R_r i_{rd} + \frac{d}{dt}\psi_{rd} - (w_s - w)\psi_{rq} \quad (3.7)$$

$$V_{rq} = 0 = R_r i_{rq} + \frac{d}{dt}\psi_{rq} - (w_s - w)\psi_{rd} \quad (3.8)$$

The stator and rotor flux linkages expressed in terms of the stator and rotor current space vectors :

$$\psi_{sd} = L_s i_{sd} + L_m i_{rd} \quad (3.9)$$

$$\psi_{sq} = L_s i_{sq} + L_m i_{rq} \quad (3.10)$$

$$\psi_{rd} = L_r i_{rd} + L_m i_{sd} \quad (3.11)$$

$$\psi_{rq} = L_r i_{rq} + L_m i_{sq} \quad (3.12)$$

The electromagnetic torque equation expressed by utilizing space vector quantities :

$$T_e = \frac{3}{2}P(\psi_{sd} i_{sq} - \psi_{sq} i_{sd}) \quad (3.13)$$

3.3.2 The $\alpha - \beta$ model equations :

After applying the a-b-c/ $\alpha - \beta$ transformation as shown in the diagram of **Figure 3.7**, we get:

$$V_\alpha + jV_\beta = \frac{2}{3}(V_a + V_b e^{\frac{j2\pi}{3}} + V_c e^{\frac{-j2\pi}{3}}) \quad (3.14)$$

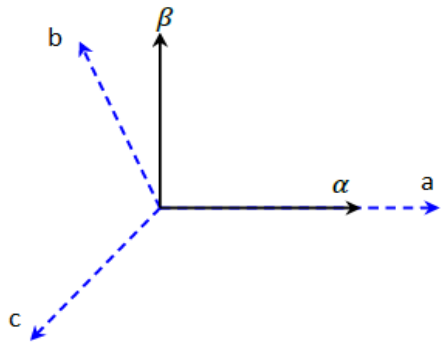

Figure 3.7: a-b-c frame to $\alpha - \beta$ frame

The AC Induction motor model is given by the space vector form of the voltage equations. The system model defined in a two-phase stationary coordinates system attached to the stator is expressed by the following equations:

The stator voltage differential equations :

$$V_{s\alpha} = R_s i_{s\alpha} + \frac{d}{dt}\psi_{s\alpha} \quad (3.15)$$

$$V_{s\beta} = R_s i_{s\beta} + \frac{d}{dt}\psi_{s\beta} \quad (3.16)$$

The rotor voltage differential equations :

$$V_{r\alpha} = 0 = R_r i_{r\alpha} + \frac{d}{dt}\psi_{r\alpha} + w\psi_{r\beta} \quad (3.17)$$

$$V_{r\beta} = 0 = R_r i_{r\beta} + \frac{d}{dt}\psi_{r\beta} + w\psi_{r\alpha} \quad (3.18)$$

The stator and rotor flux linkages expressed in terms of the stator and rotor current space vectors :

$$\psi_{s\alpha} = L_s i_{s\alpha} + L_m i_{r\alpha} \quad ((3.19)$$

$$\psi_{s\beta} = L_s i_{s\beta} + L_m i_{r\beta} \quad (3.20)$$

$$\psi_{r\alpha} = L_r i_{r\alpha} + L_m i_{s\alpha} \quad (3.21)$$

$$\psi_{r\beta} = L_r i_{r\beta} + L_m i_{s\beta} \quad (3.22)$$

The electromagnetic torque equation expressed by utilizing space vector quantities :

$$T_e = \frac{3}{2}P(\psi_{s\alpha} i_{s\beta} - \psi_{s\beta} i_{s\alpha}) \quad (3.23)$$

3.4 Water Pump

3.4.1 Pump types

The pumps used in small water systems can be divided into two general categories. The basic difference between the two types is their response to changes in discharge pressure. [13]

- **Dynamic pumps:**

Dynamic pumps are used in conditions where high volumes are required and a change in flow is not a problem. As the discharge pressure on a dynamic pump is increased, the quantity of water pumped is reduced. One type of dynamic pump, centrifugal pumps, arc the most common pump used in water systems. Dynamic pumps can be operated for short periods of time with the discharge valve closed.

- **Displacement pumps:**

Displacement pumps are used in conditions where relatively small, but precise, volumes are required. Displacement pumps will not change their volume with a change in discharge pressure. Displacement pumps are also called positive displacement pumps. The most common positive displacement pump is the diaphragm pump used to pump chlorine and fluoride solutions. Operating a displacement pump with the discharge valve closed will damage the pump.

3.4.2 Centrifugal Pump

The water pump commonly found in our systems is centrifugal pumps. These pumps work by spinning water around in a circle inside a cylindrical pump housing. The pump makes the water spin by pushing it with an impeller. The blades of this impeller project outward from an axle like the arms of a turnstile and, as the impeller spins, the water spins with it. As the water spins, the pressure near the outer edge of the pump housing becomes much higher than near the center of the impeller.

A centrifugal pump has two main components shown in **Figure 3.8**

- A rotating component comprised of an impeller and a shaft .
- A stationary component comprised of a casing, casing cover, and bearings .

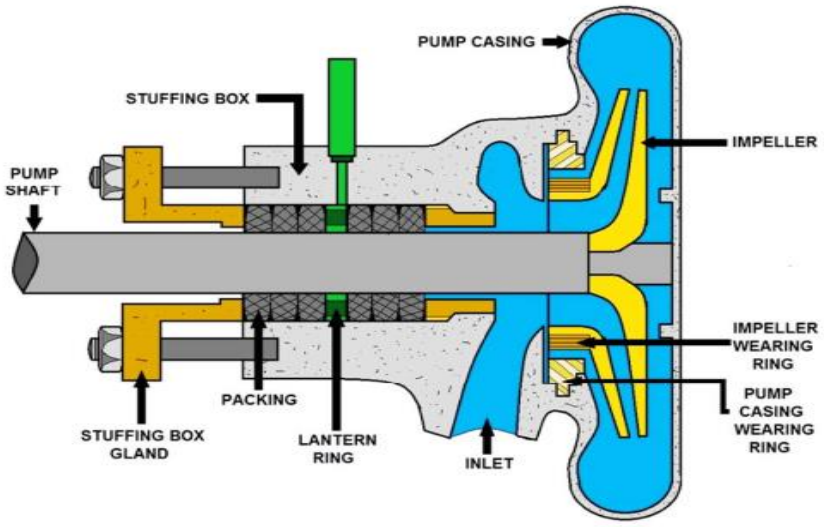

Figure 3.8: Centrifugal Pump Parts [13]

3.5 Field Orientated Control

The Field Oriented Control (FOC) consists of controlling the stator currents represented by a vector. This control is based on projections which transform a three-phase time and speed dependent system into a two co-ordinate (d and q co-ordinates) time invariant system. [14]

Figure 3.9 shows a block diagram of the field oriented control system (hysteresis FOC) for induction motor . The stator quadrature-axis reference is calculated from torque reference input (Γe^*) as :

$$i_{sq} = \frac{Lr}{pM}\left(\frac{\Gamma e*}{|\psi_r|}\right) \qquad (3.24)$$

The estimated rotor flux linkage Ψˆ r is given by:

$$|\psi_r| = \frac{M}{Tr.S+1}\, i_{sd} \qquad (3.25)$$

The stator direct-axis current reference is obtained from the rotor flux reference *

$$i_{sd}{}^{*} = \frac{|\psi_r|^{*}}{M} \tag{3.26}$$

The ωs required for coordinates transformation is generated from the rotor speed ωr and slip frequency ωsl:

$$\omega s = \omega sl + p\Omega r \tag{3.27}$$

The latter is obtained from the stator reference current isq*

$$\omega sl = \frac{M}{|\psi_r|}\left(\frac{1}{Tr}\right) i_{sq}{}^{*} \tag{3.28}$$

The current isq* and isd* are converted into phase current references ia* , ib* , ic* . The regulators process the measured and reference currents to produce the inverter gating signals Sa , Sb , Sc

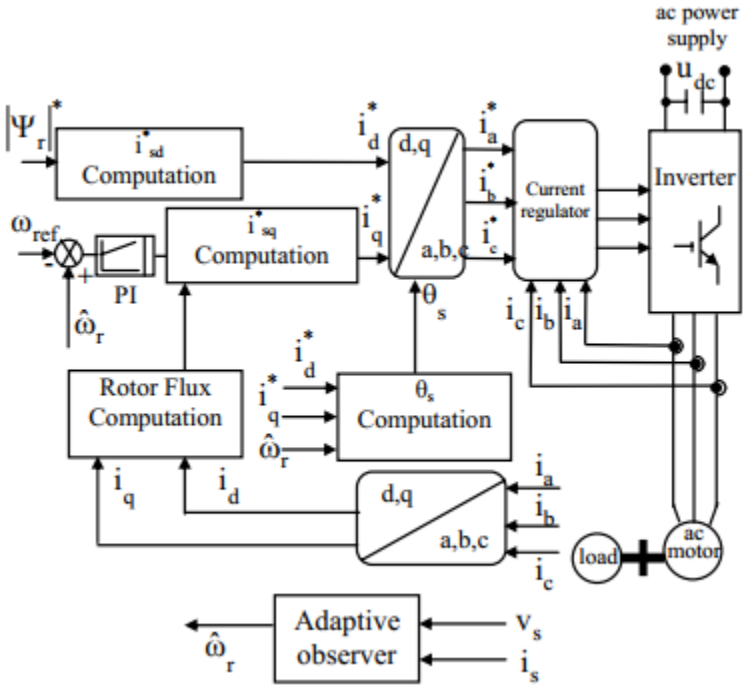

Figure 3.9: Basic indirect field-oriented control for induction motor drives

3.6 Conclusion

This chapter was dealt with induction motor, its construction, principle of operation and mathematical model. The different types of water pumps were presented, also the hysteresis field oriented control method has been used to control the induction motor .

Chapter Four

Simulation and Results

4.1 Introduction

In this chapter, the simulation of the water pumping PV system will be discussed. In the first part, how to build and analyze the simulation model of the MPPT system, and two level inverter. The simulations were built in MATLAB / Simulink independently; the simulation model mainly consists of the power circuits and the control circuits.

Then the simulation results of the three phase induction motor controlled by hysteresis field oriented control are shown and analyzed.

Finally, we finish this chapter with a simulation of the whole system

4.2 Simulation of MPPT

Using MATLAB/SIMULINK, we have done the simulation for the PV system with MPPT controller. **Figure.4.1** shows the solar MPPT with resistive load(30ohm) circuit. It contains a PV panel, buck-boost converter and the MPPT controller circuit.

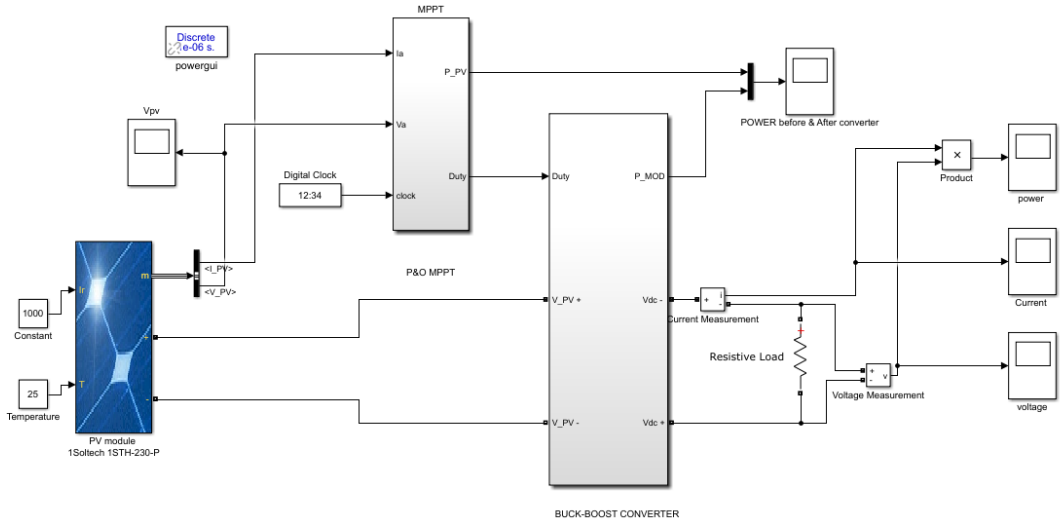

Figure 4.1: Double-stage MPPT system simulation model.

The content of the buck-boost converter is shown in the **figure 4.2**

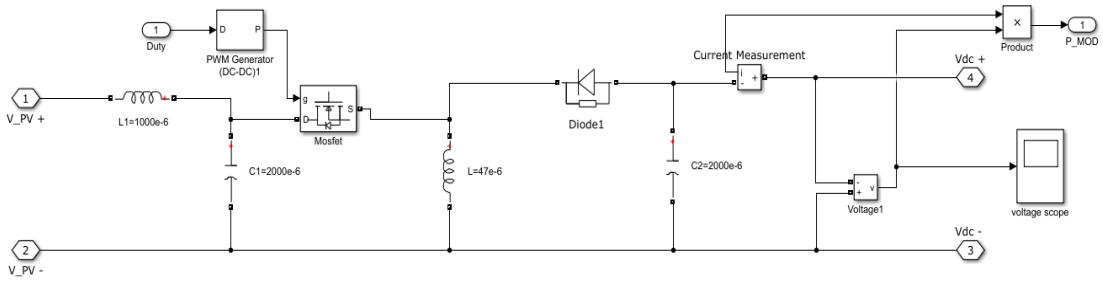

Figure 4.2: Buck-boost converter simulation model.

4.2.1 Simulation Results

The simulation results are obtained at the ideal atmospheric conditions T=25°C, G=1000W/m2.

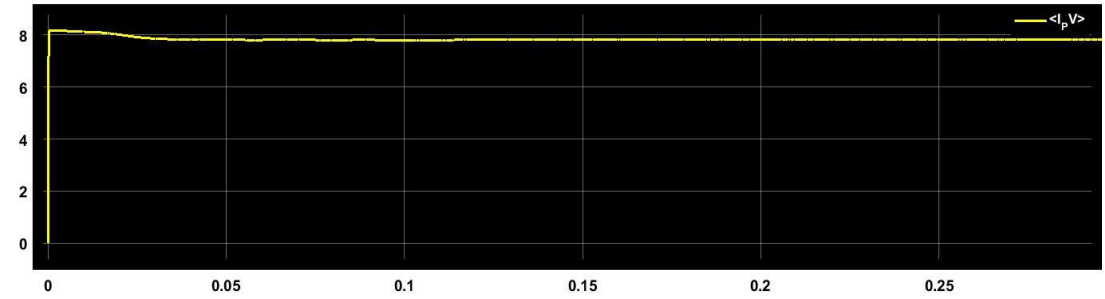

Figure 4.3: The PV current.

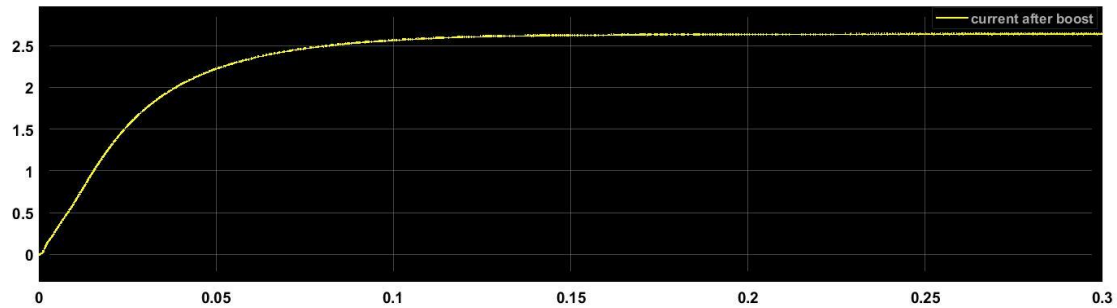

Figure 4.4: The output current of the buck-boost

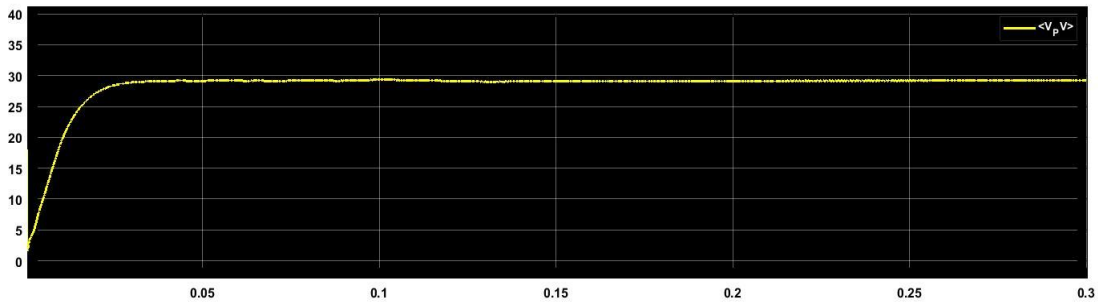

Figure 4.5: The PV voltage.

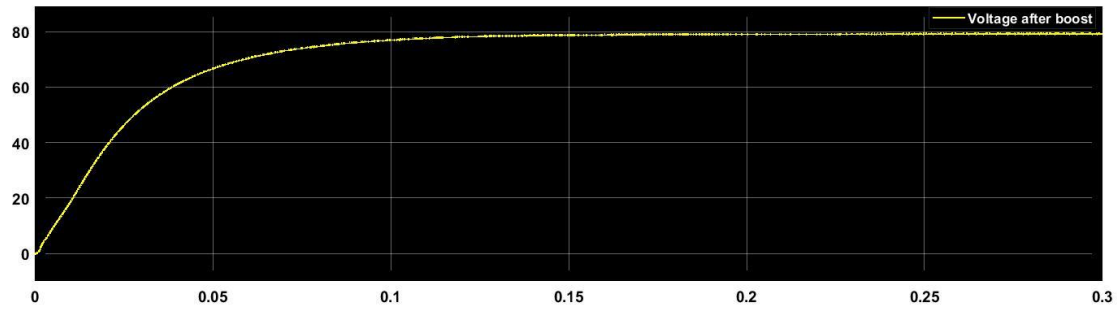

Figure 4.6: The output voltage of the buck-boost.

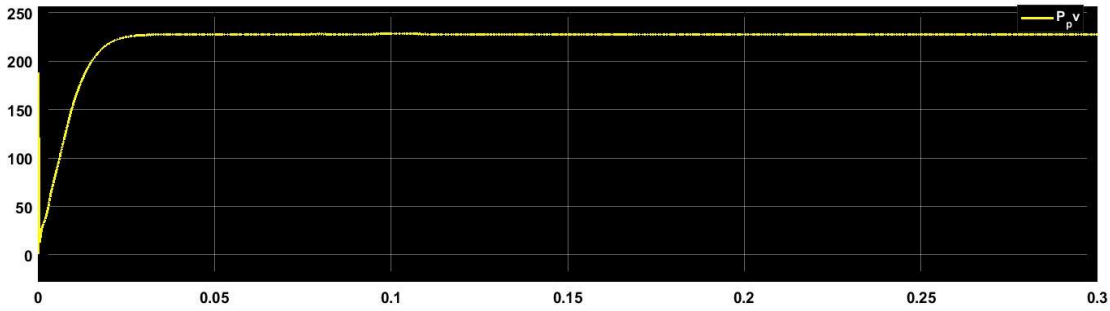

Figure 4.7: The PV Power.

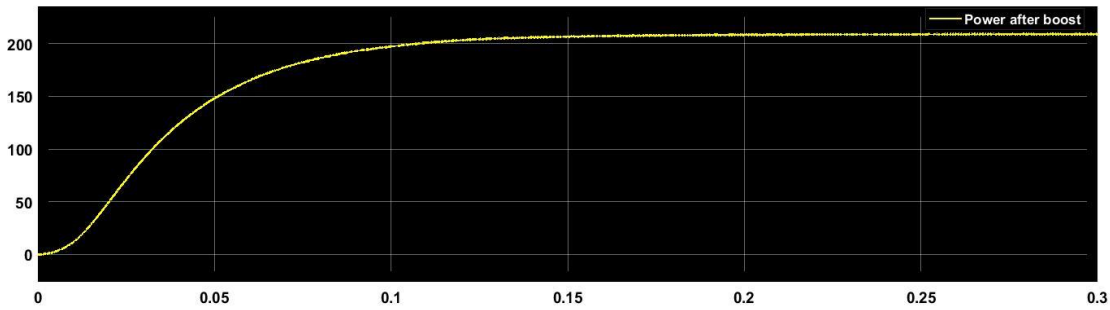

Figure 4.8: The output Power of the buck-boost.

4.2.2 Discussion

The used PV array is 1Soltech 1STH-230P, it consists of 1 Parallel string containing 1 Series-connected module.

When the temperature is 25°c and the irradiation is 1000W/m2, we get the following results:

- The output power (Pout) is 209 W.
- The panel power (P_{PV}) is 228 W.
- The output voltage (Vout) is 79.2 V.
- The panel voltage (V_{PV}) is 29.2 V.
- The output current (Iout) is 2.64 A.
- The panel current (I_{PV}) is 7.8 A.
- The efficiency =Pout/Ppv=209W/228W=0.917.
- The panel voltage (Vpv) is approximately as the value in the data sheet of the solar panel we used.
- The panel current (Ipv) is approximately as the value in the data sheet of the solar panel we used.

4.3 Simulation of two level inverter

A three phase two-level inverter can be configured by using a six IGBT switches controlled by hysteresis subsystem as shown in Simulink circuit in **Figure 4.9**.

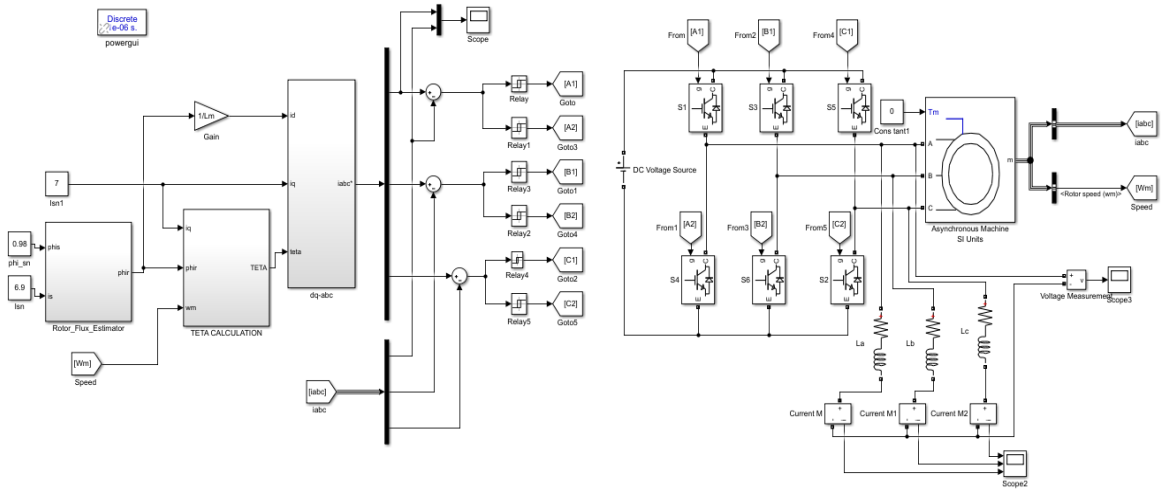

Figure 4.9: Simulink circuit for three phase two-level inverter controlled by hysteresis

4.3.1 Simulation parameters:

Power of the motor: 3kw
V_{dc} = 600V
Resistance of RL branch: 50 ohms
Inductance of RL branch: 10 mH

The output results of simulation are shown below:

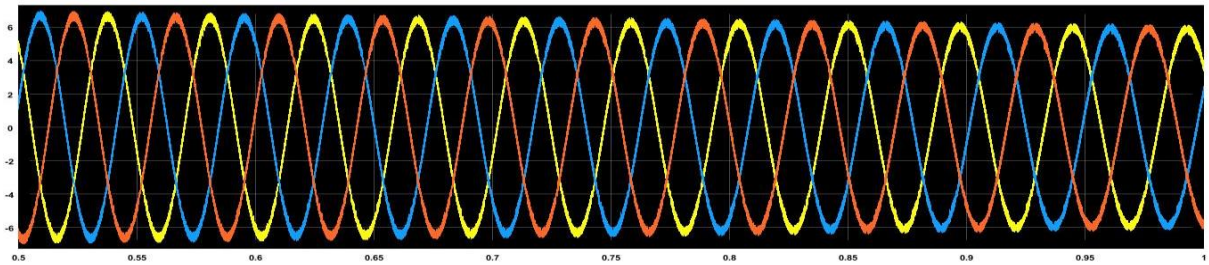

Figure 4.10: Three phase output current of two level inverter controlled by hysteresis

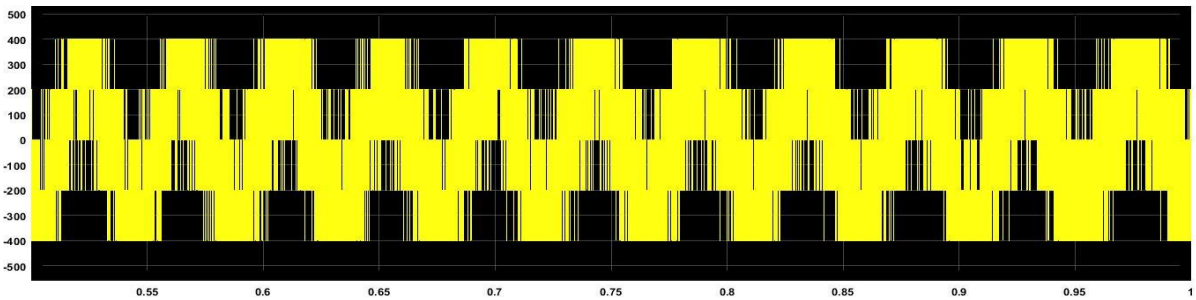

Figure 4.11: Three phase output Line-Neutral voltage of two level inverter controlled by hysteresis

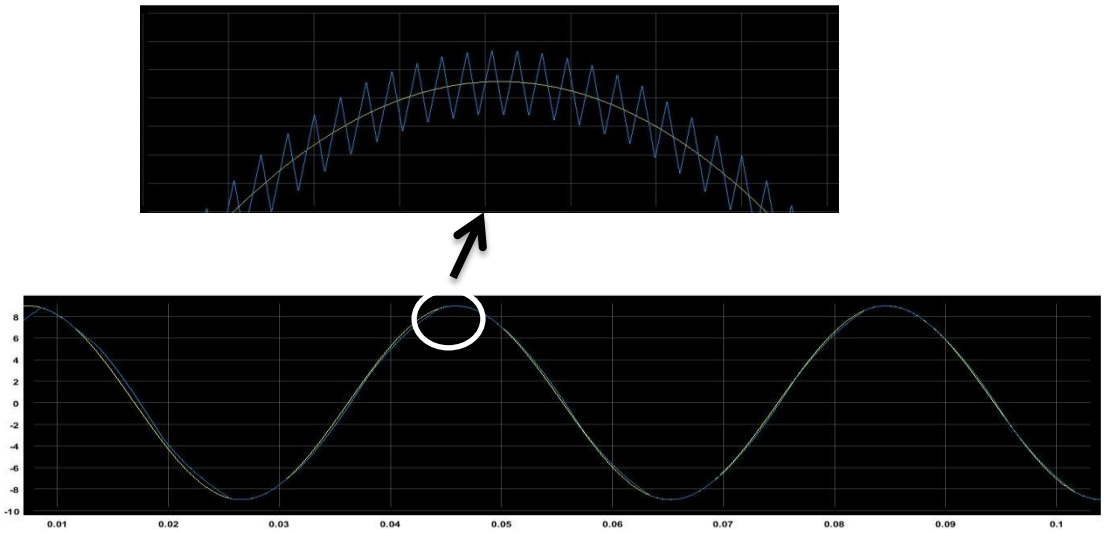

Figure 4.12: The output of the hysteresis control

4.3.2 Discussion

Figure 4.10 shows three phase output current of two level inverter controlled by hysteresis which mostly sinusoidal.

Figure 4.11 shows three phase output Line-Neutral voltage of two level inverter controlled by hysteresis, where its peak value is 400V (2/3 V_{dc}).

Figure 4.12 shows the output of the hysteresis control, where the measured current is follow the reference one in an interval of 0.001.

4.4 Simulation of field oriented control of induction motor

Using MATLAB/SIMULINK, we have done the simulation for the induction motor controlled by field oriented hysteresis control. **Figure 4.13** shows the simulation blocks.

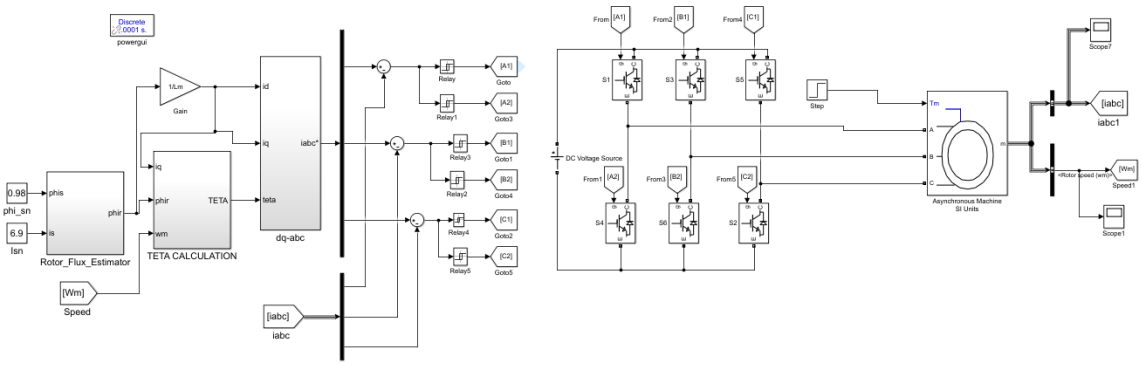

Figure 4.13: Simulation of the induction motor controlled by FOC hysteresis control

4.4.1 Simulation parameters

Motor parameters:

Table 4.1 : Parameters of 3KW induction motor

Power	Pn=3000W
Voltage	Vn=380V
Current	In=6.9A
Frequency	*Fn=50Hz*
Number of pole pairs	Pb=2
Moment of inertia	J=0.007Kgm2
Stator winding resistance	*Rs* = 1.85Ω
Rotor winding resistance	*Rr* = 1.84Ω
Stator inductance	*Ls* = 170 mH
Rotor inductance	*Lr* = 170 mH
Mutual inductance	*LM* = 160 mH

4.4.2 Simulation Results

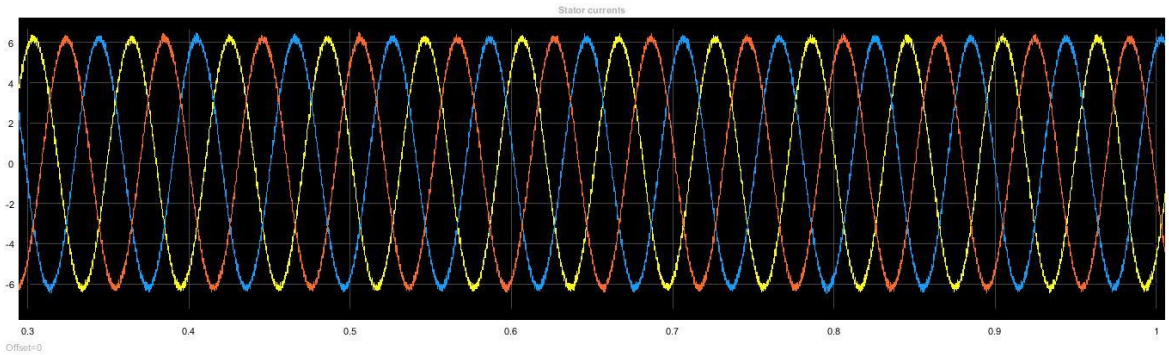

Figure 4.14: Stator currents

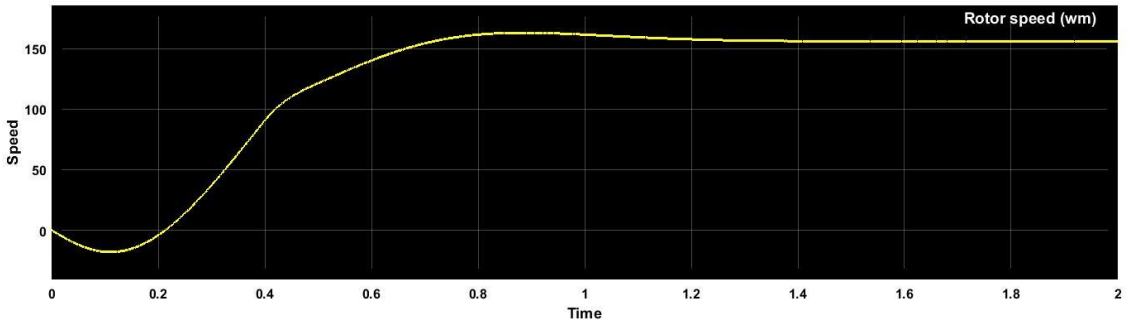

Figure 4.15: Rotor Speed

4.4.3 Discussion

Figures 4.14 shows the stator currents of three phase induction motor with a peak value of 6.45 A, which is mostly sinusoidal waveform

Figure 4.15 shows the Rotor speed with a value less than 200rad/s .

4.5 Simulation of the whole system

After doing the simulation of each part alone, in this section we will simulate the whole system together.

Using MATLAB/SIMULINK, we have done the simulation for the whole system. **Figure 4.16** shows the simulation blocks.

é

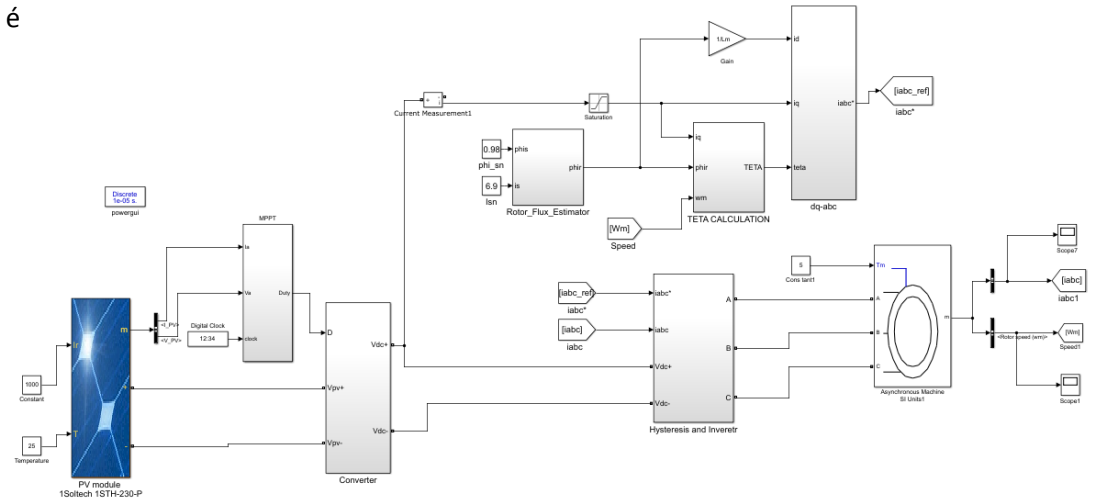

Figure 4.16: Simulation of the whole system

4.5.1 Simulation Results

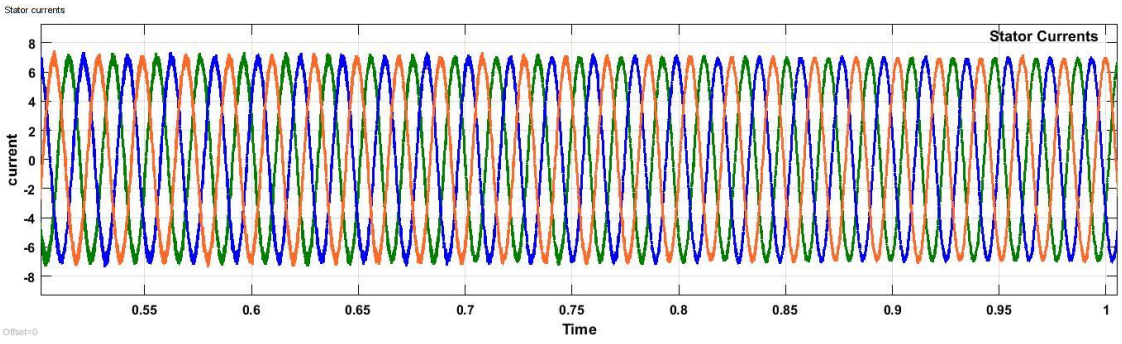

Figure 4.17: Stator currents

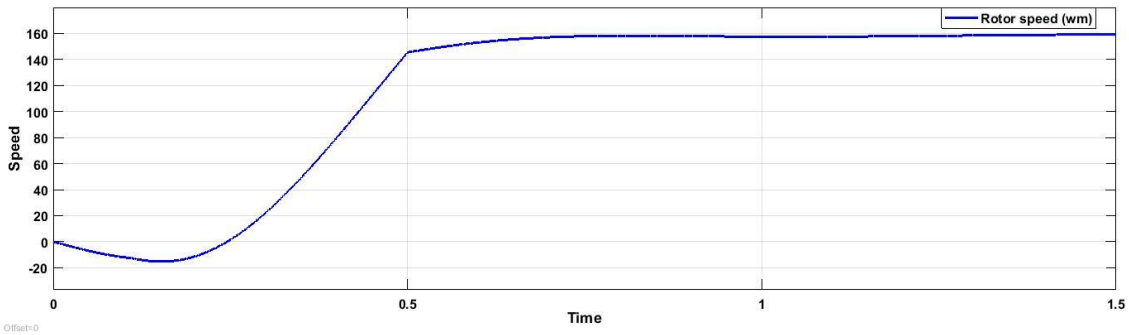

Figure 4.18: Rotor Speed

4.5.2 Discussion

Figure 4.17 shows the stator currents at the steady state which is mostly sinusoidal.

Figure 4.18 shows the rotor speed which reaches the rated seed.

This result is obtained by using a step to the load input with an initial value equals to ‘1’ and a final value equal to ‘5’ in a step time of ‘0.5’.

4.6 Conclusion

In this chapter, water pumping PV system three-phase was investigated and analyzed. The proposed system consists MPPT model, two level inverter and induction motor controlled by field oriented hysteresis control.

Chapter Five

Implementation

5.1 Introduction

This chapter deals with the experimental set up of the main part of our project which is the implementation of the open and closed loop hysteresis field oriented control of three phase induction motor ,based on the background introduced in the previous chapters and the simulation done in chapter four to consolidate the theoretical analysis of this thesis.

The experimental work was conducted in the Power Research Laboratory at the Institute of Electrical and Electronic Engineering of Boumerdes University. The implementation is conducted for a three-phase squirrel cage 1.8kW induction motor using a DSP TMS320F2833x as a microcontroller.

5.2 Operation description

To assess the control strategy presented in this thesis in real time, an experimental test bench shown in Figure 5.1 is built. The present work consists of a 3-phase power supply supplying a **Semikron didactic** inverter, feeding a 1.8 kW 4 poles squirrel cage induction motor. The control algorithm is implemented via a **DSP TMS320f2833x Piccolo** from Texas Instruments. The connection between the micro-controller and the power converter is carried out by an interface card that adapts the control signal levels called the **Dspace** from Micro Technologies Lab Company. The main role of this card is to separate between the low power side and the high power side in order to protect the micro-controller. The different current measurements' are ensured by current sensor circuits using LA55P hall effect sensors. These current circuits are used essentially to measure the actual current for both phases a and b under any operating condition and then are used to compute the (d, q) current components in the rotating (d, q) reference frame. In order to monitor the different obtained results a numerical oscilloscope **Gwinstek GDS-1042** has been used .

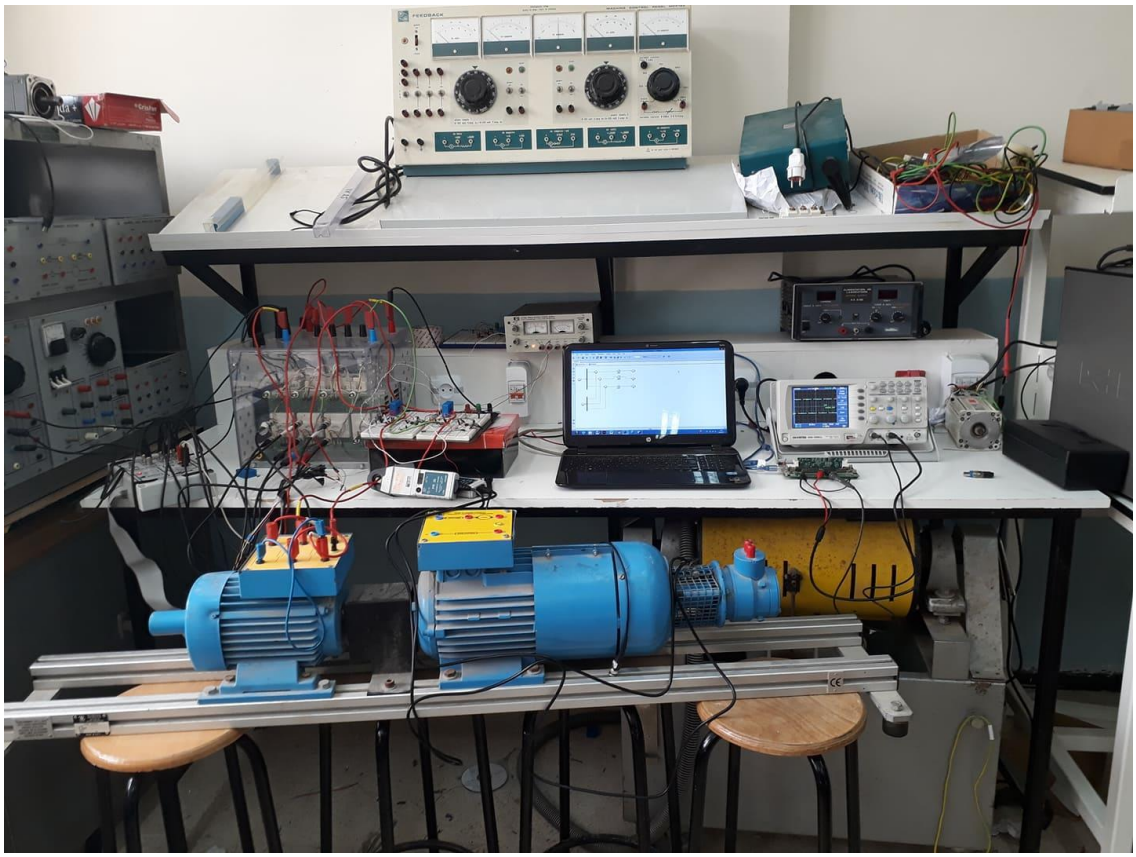

Figure 5.1: Implemented test bench of the hysteresis Field Oriented Control

5.3 Material used for implementation

To do our implementation we need a lot of materials and components, in this part we introduce the most important materials used.

Induction Motor

The three phase induction motor used in the implementation is shown in the **figure 5.2,** and its parameters are shown in the **table 5.1**:

Table 5.1: Parameters of the induction motor

Power	1.8KW
Frequency	50 Hz
Current	3.8A/5A
Voltage	380V/400V
Stator Resistance	5.06 ohm
Rated Speed	1500

Figure 5.2: Three phase induction motor

Semikron Inverter

Semikron inverter is a three phase IGBT two level inverter (Three phase voltage supply 400, Nominal current 30A)

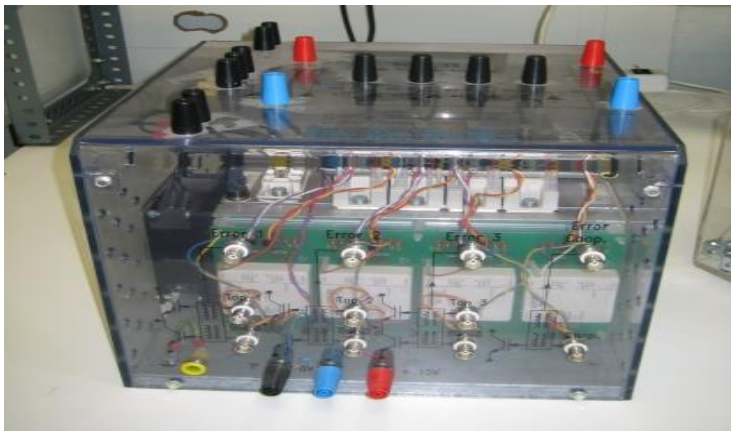

Figure 5.3: Semicron Inverter

Dspace interface board

Dspace interface it is a Micro-technologies Lab equipment. It is an adaptation and isolation interface which separates between the high power and the low power side in order to protect the micro-controllers

Figure 5.4: Dspace from Micro Technologies

DSP TMS320F2833x

TMS320F2833x devices, members of the TMS320C28x/ Delfino™ DSC/MCU generation, are highly integrated, high-performance solutions for demanding control applications.

Figure 5.5: DSP TMS320F3328x

The hysteresis field oriented control algorithm was implemented using DSP TMS320F2833x card.

In order to program this card, we have used MATLAB/Simulink C2000 tools.

5.4 Algorithms of the hysteresis field oriented control

In this part we talk about the schematic and the diagram circuits of this control using Simulink/Matlab program.

5.4.1 Open loop current control

The algorithm of the open loop hysteresis field oriented control was build using Simulink. **Figure.5.6** illustrates a Simulink diagram circuit for this control strategy.

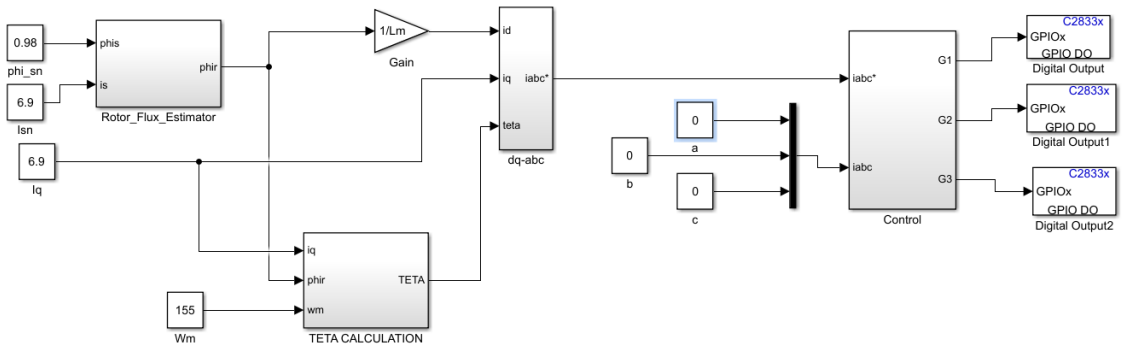

Figure 5.6: Simulink block diagram of the open loop hysteresis FOC for DSP

As we see in the **Figure 5.6**, digital outputs are used and uploaded to the GPIO pins. GPIO is the abbreviation of General-Purpose Input/Output. which is an uncommitted digital signal pin on an integrated circuit or electronic circuit board whose behavior is controllable by the user at run time (including whether it acts an input or output).

5.4.2 Closed loop current control

The algorithm of the closed loop hysteresis field oriented control was build using Simulink. **Figure.5.7** illustrates a Simulink diagram circuit for this control strategy.

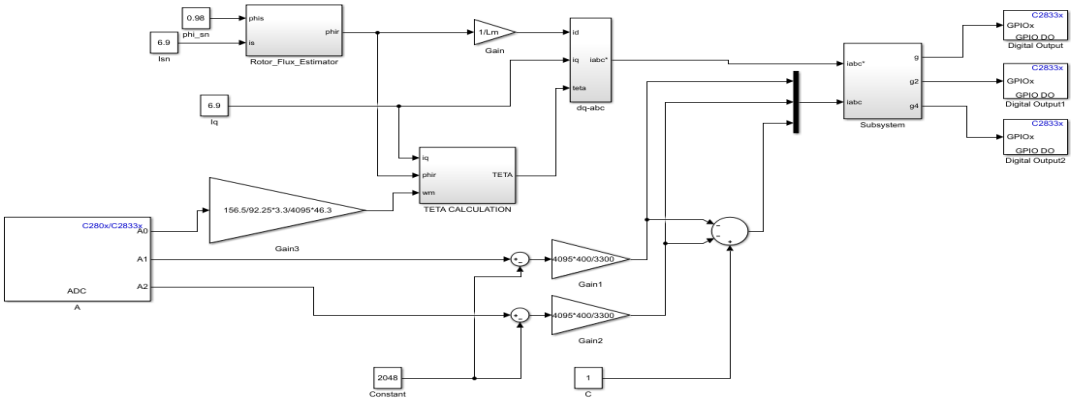

Figure 5.7: Simulink block diagram of the closed loop hysteresis FOC for DSP

The main difference between the open and the closed loop is the feedback currents and speed, for that we need the ADC block to covert these analog quantities into digital ones.

5.4.2.1 ADC configuration :

In this implementation, three ADCs have been used which areADCINA0, ADCINA1 and ADCINA3.

These ADCs were used in order to measure:

- Induction motor Currents (phase a , and phase b)
- The speed from the tachometer.

The used DSP ADCs can accept a voltage between [0-3]V , therefore a software compensation must be added in order to remove the incorrectness of the read value. Thus, a calibration of the ADC is a must.

Calibration of the ADC of DSP TMS320F2833x :

Analog to digital converter with no error in both the gain and the offset follows a linear law expressed as follow:

$$Y = xm_i \qquad (5.1)$$

Where $m_i$is the ideal gain generally is 1.

$$x = \text{input voltage} * \frac{4095}{3\,V} \qquad (5.2)$$

where x is the input signal.

But in reality there is no ideal gain when using a hall effect sensor; so the exact expression of the signal is as follows:

$$Y = x * m_a + b \qquad (5.3)$$

Where m_a is the actual gain, and b is the actual offset.

5.4.2.2 Current sensor circuit :

LEM LA55-P hall effect transducer was used in order to sense the current. its ratio of the input current over the output current is (1/1000) . Its circuit is depicted in **Figure.5.5.**

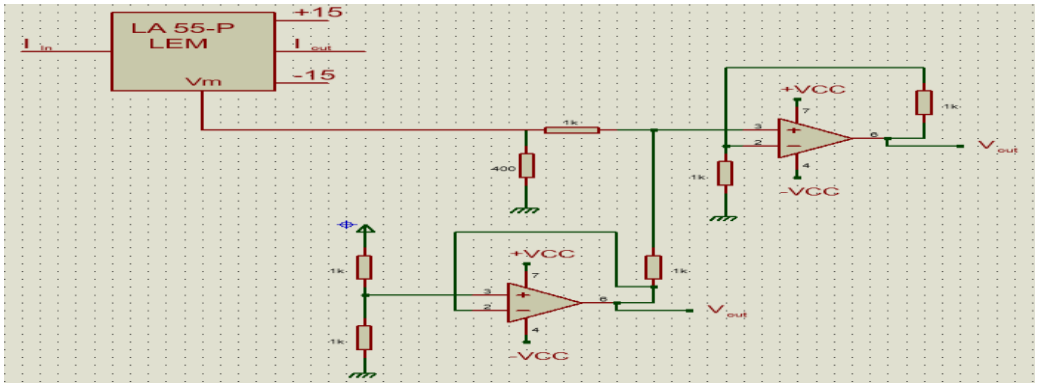

Figure: 5.8 - Current sensor circuit

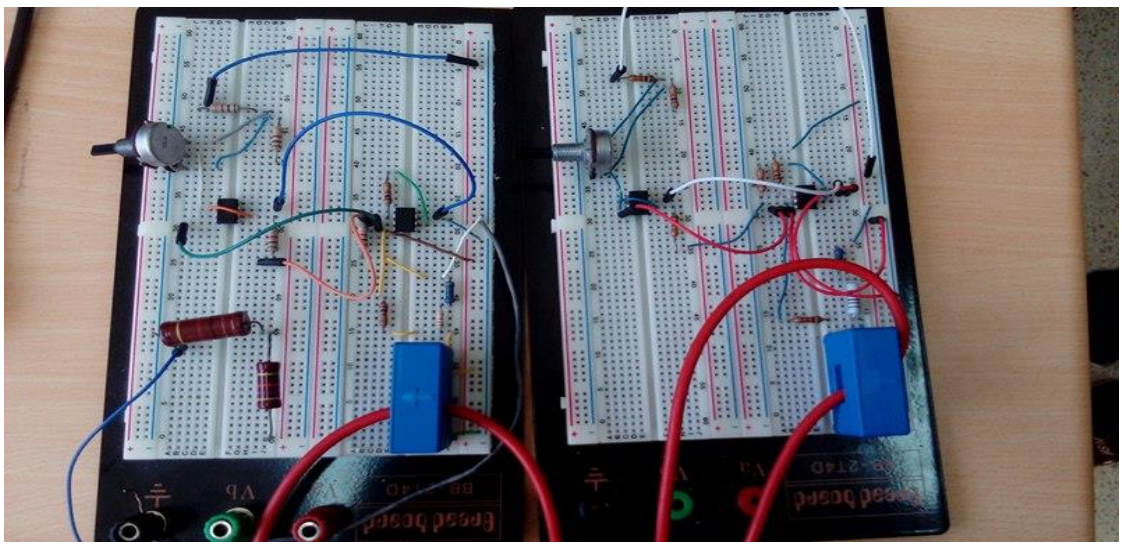

Figure 5.9: Implemented current sensor circuit

From **Figure 5.9**, we can notice that two hall effect current sensor circuits were built in order to sense two phases of the motor current ia and ib. Whereas the third phase ic is estimated using the software (ic=-ia-ib).

5.5 Implementation results :

After the experimental test bench shown in **Figure 5.1** is built, and the Similink program shown in the **Figure 5.6** is uploaded to the DSP we get the following results:

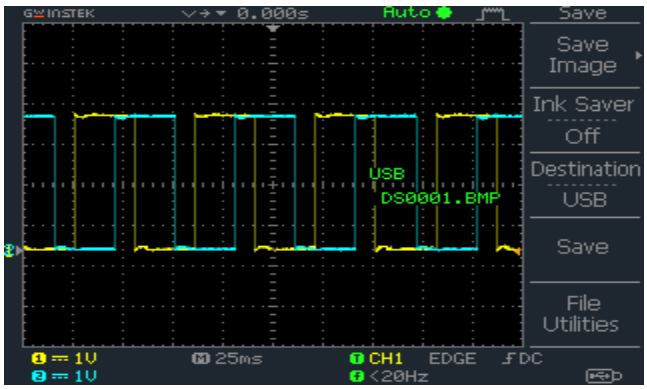

Figure 5.10: Generated PWM

Figures 5.10 shows the generated PWM from the DSP as the output of GPIO pins, which has a duty cycle of 50%.

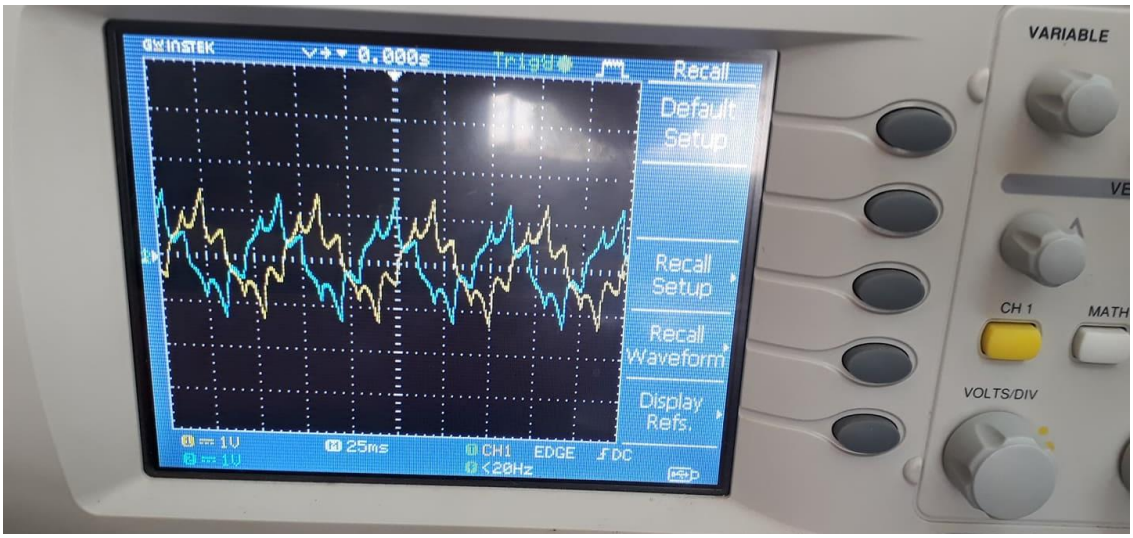

Figure 5.11: Stator currents (Ia,Ib)

Figure.5.11 shows the input currents' curves '$\mathbf{I_a}$' and '$\mathbf{I_b}$' that have a phase shift between them equal to $2\pi/3$,also we can notice that the currents have many harmonics which is the limitation of this technique.

Figure 5.12 - Stator flux components

Figure 5.12 shows the rotor spped, which is measured by the Photo-Tachometer

5.6 Conclusion :

This chapter covered the implementation setup and results of the open and closed loop hysteresis field oriented control of three phase induction motor

It has been noticed that both the implementation and simulation results are in perfect match .

Furthermore, from this implementation it can be concluded that this technique is like a sensorless technique as the control of the motor could be achieved even without using the feedback parameters.

General Conclusion

In this work a three-phase double stage water pump interactive inverter with maximum power point tracking capability is analyzed, designed, simulated and part of it is implemented. The goal of our work was to extract the maximum power from the panel, convert it to AC power then inject it into a 3 phase induction motor . The proposed PV system consists of two-level inverter, buck-boost chopper and prevents DC current injection. The reference voltage of the inverter is set by proposed MPPT algorithm in order to draw the possible highest power from PVs all the time. **the Perturb and Observe (P&O)** method is used, which is adapted for double stage inverter. It seems from the simulation results that the inverter output current is almost sinusoidal waveform.

Also, a 3 phase induction motor has been controlled using field oriented control . Since only one inverter is used for all of the procedures such as water pump interactive operation and MPPT, the size and the cost of the system are decreased and total efficiency is increased. In the implementation part, just an open loop three-phase induction motor using field oriented control technique is implemented, which represents the largest hardware part of the whole system. Experimental tests have shown the effectiveness and capability of using TMS320F2833X board in controlling such a complex system; control of three-phase induction motor .

‘Our imagination is the only limit to what we can hope to have in the future.’

Charles F. Kettering

References

[1] N. A. I. S. Saban Ozdemir, Single stage three level grid interactive MPPT inverter for PV systems, Energy Conversion and Management: 561–572 , 2014.

[2] S. I. Altin N, dSPACE based adaptive neuro-fuzzy controller of grid interactive inverter, Energy Convers Manage: 56:130–9., 2012.

[3] D. M. Ç. I. Sefa I, Application of one-axis sun tracking system, Energy Convers Manage: 50:2709–18., 2009.

[4] Djamila Rekioua • Ernest Matagne, Optimization of Photovoltaic Power Systems, Modelization, Simulation and Control

[5] R. Y. M. F. Habbati Bellia, A detailed modeling of photovoltaic module using MATLAB, Volume 3 Issue 1 Pages 53–61., June 2014.

[6] E. E. S. J. S. A. H. M.B. Eteiba, A Photovoltaic (Cell, Module, Array) Simulation and Monitoring Model using MATLAB®, (0975 – 8887) Volume 69– No.6.

[7] Mirjana Milosevic, Hysteresis Current Control in Three-Phase Voltage Source Inverter

[8] ABD ALMULA G. M. GEBREEL, Simulation And Implementation Of Twolevel And Three-Level Inverters By Matlab And Rt-Lab, 2011

[9] A. A. G. M. Gebreel, simulation and implementation of two level and three-level inverters by matlab and rt-lab, the ohio state university, 2011.

[10] Reza Davoodnezhad, Hysteresis Current Regulation Of Voltage Source Inverters With Constant Switching Frequency

[11] Abdel-Karim Daud, Basim Alsayid, Arafat Zaidan, DSP Based Simulator for Field Oriented Control of the Surface Permanent Magnet Synchronous Motor Drive, Issue 1, Volume 6, 2012

[12] Stephen J. Chapman, Electric Machinery Fundamentals, Fifth Edition

[13] www.abctlc.com, Pumps And Motors Continuing Education Professional Development Course

[14] M. S. Merzoug, and F. Naceri, Comparison of Field-Oriented Control and Direct Torque Control for Permanent Magnet Synchronous Motor (PMSM), World Academy of Science, Engineering and Technology 21, 2008